A Monte Carlo Study of Isomers and Structural Evolution in Benzene−Cyclohexane Clusters: $(C_6H_6)(C_6H_{12})_n$, $n = 3-7, 12$

David C. Easter,* Jessica A. Roof, and Laura Jeanne Butts

Department of Chemistry and Biochemistry, Texas State University, San Marcos, Texas 78666

Received: July 4, 2007; In Final Form: October 5, 2007

Monte Carlo simulated annealing strategies, carried out on four different potential energy surfaces, are applied to benzene−cyclohexane clusters, BC_n, $n = 3-7$, 12, to identify low-energy isomers and to trace the evolution of structures as a function of cluster size. Initial structures are first heated to ensure randomization, and subsequent annealing yields optimized rigid, low-energy clusters. Five major structural isomers are identified for BC_3: one assumes the form of a symmetric, modified sandwich; the remaining four lack general symmetry, assuming distorted tetrahedral arrangements. For BC_4 and larger clusters, the number of low-temperature isomers is large. It is, nevertheless, feasible to classify isomers into groups based on structural similarities. The evolution of BC_n structures as a function of cluster size is observed to follow one of two primary paths: The first maximizes benzene−cyclohexane interactions and places benzene in or near the BC_n cluster center; the competing path maximizes cyclohexane−cyclohexane interactions and distances benzene from the cluster's center of mass. Results for BC_3 and BC_4 are discussed with reference to experimental results and models previously applied to interpret benzene−argon cluster spectra.

I. Introduction

Properties and dynamics of molecular clusters are of fundamental interest because of the unique role that clusters play in linking isolated molecules to bulk liquids and solids. Clusters possess unique, size-specific properties that evolve in some fashion as a function of cluster size. In recent years, neat benzene clusters have received both experimental[1−11] and theoretical[12−18] attention, bringing significant new information to light regarding neat aromatic cluster systems. To extend the benzene cluster work, benzene−cyclohexane clusters (BC_n) that contain a single C_6H_6 moiety have been of interest, partially because experimental and computational results from BC_n can be compared directly to $(C_6H_6)(C_6D_6)_n$ data. Both solvents, C_6H_{12} and C_6D_6, have identical molecular masses, eliminating mass dependence as a factor in side-by-side comparisons. In addition, when probed in the appropriate region, the experimentally observed C_6H_6 $B_{2u} \leftarrow A_{1g}$ vibronic transitions (0_0^0 and 6_0^1) are well-separated from spectroscopic absorptions of the C_6H_{12} solvent, providing a sensitive method to probe the environment of the C_6H_6 chromophore and to identify cluster properties.

More than two decades ago Hoare elucidated a structural shell-filling growth sequence for van der Waals clusters composed of spherical (nonpolar) molecules or atoms, for example, argon clusters, Ar_n.[19] The sequence includes an equilateral triangle ($n = 3$), tetrahedron ($n = 4$), trigonal bipyramid ($n = 5$), octahedron ($n = 6$), pentagonal bipyramid ($n = 7$), hexagonal bipyramid ($n = 8$), and icosahedron ($n = 13$). Some molecular clusters of nonspherical nonpolar molecules have been hypothesized to partially mimic the same sequence.[20] For such lower-symmetry systems (e.g., benzene−cyclohexane clusters), some deviation from Hoare's structures is inevitable; nevertheless, those structures provide a useful reference to which the BC_n structures have historically been compared.[20]

El-Shall and Whetten reported one-color resonant two-photon ionization (R2PI) spectra of BC_n clusters measured through the 6_0^1 vibronic transition of benzene.[20] Their data were interpreted in support of a structural shell-filling model, and the two sharp features in the BC_6 spectrum were tentatively assigned to a C_6H_6 chromophore occupying one of two distinct positions—axial or equatorial—within a pentagonal bipyramid structure.

We recently reported one-color R2PI $B_{2u} \leftarrow A_{1g}$ 6_0^1 spectra of BC_n clusters, $n = 1-10$.[21] The $n = 1-3$ spectra are dominated by van der Waals progressions, and most of the larger-sized clusters have only a few sharp features. Subsequently, we also reported the results of a Monte Carlo simulated annealing (MCSA) investigation focusing on low-temperature isomers of the dimer (BC_1) and trimer (BC_2).[22] A single parallel-displaced isomer was identified for BC_1, which—supported by an MP2 frequency calculation—nicely accounts for the van der Waals mode in the BC_1 spectrum. Eight independent isomers were identified for BC_2: Three assume a parallel-stacked (sandwich) arrangement, while five assume trigonal arrangements. The isomer distribution is consistent with the pair of van der Waals progressions observed in the BC_2 vibronic spectrum, which were tentatively assigned separately to each of the two isomeric groups—one progression representing the sandwich group, and the other originating from the trigonal group.

In this report we expand the previous computational study to include BC_n, $n = 3-7$, 12. Motivation for doing so includes a desire to address the following questions: (1) Are there a small number of isomers for these cluster sizes and—if not—at what cluster size does the number of isomers first become large? (2) Are isomeric structures and/or structural groups useful in explaining the experimental BC_n spectra? (3) What fraction of isomers approximate the model structures identified by Hoare? (4) Is it possible to identify a growth sequence that describes the evolution of BC_n cluster structures as a function of size?

* Author to whom correspondence should be addressed. E-mail: de05@txstate.edu.

10.1021/jp075214i CCC: $37.00
Published on Web 11/29/2007

(5) Can the experimental spectra be interpreted in terms of calculated structures and an interpretation model previously applied to benzene−argon clusters?

II. Computational Approach

We previously described and documented a comprehensive strategy for generating and identifying isomers of small benzene−cyclohexane clusters.[22] Because the approach of this study is fundamentally similar, we provide here only an overview of the process. Reference 22 should be consulted for complete detail.

II.A. Generation of Cold Structures. Several initial configurations were generated for each cluster size $(C_6H_6)(C_6H_{12})_n$, $n = 3-7$, by starting with an unoptimized $n - 1$ cluster structure and adding one cyclohexane molecule in a random position and orientation. These initial structures were typically heated from 2 to 200 K in 100 temperature steps, each consisting of 10^4 isothermal Monte Carlo trial moves. The hot structures were then cooled, first to 1 K and then to 0.01 K in sequential stages—both of which typically utilized 200 temperature steps consisting of 10^4 Monte Carlo (MC) moves each. Optimization is achieved in the final cooling stage.

The reported structures represent the minimum-energy (not final or average) structures encountered during the simulation. Such minimum-energy structures are normally encountered during the final temperature step (0.01 or 0.001 K). Results are consistently repeatable: For example, energy minima are reproducible to six or more significant digits—far more than are physically meaningful. Our calculations on B_{13} clusters via this technique[12,13] either matched or improved upon previously reported results.[15−18] Recent state-of-the-art calculations have verified the minimum energies of our B_{13} calculations but were incapable of improving upon them.[35]

Variations on the basic sequence were applied to individual cluster sizes. For BC_3, all heating and cooling stages used 1000 T steps consisting of 2×10^4 MC moves, with a final optimization temperature of 0.001 K. For BC_4, the warming stage was carried out in 200 temperature steps. For BC_5, initial configurations were created by adding two cyclohexane molecules to BC_3 structures, and the heating stage involved 200 temperature steps. For BC_7, configurations were cooled only to 1 K. For BC_{12}, the initial configuration was adapted from the published B_{13} C_3 structure,[12] except that all distance (R) coordinates were increased by 25%. This configuration was warmed in separate runs on the four potential energy surfaces (PESs) in two stages: first from 1 to 200 K in 200 steps (10^4 MC moves), then from 200 to 300 K in 201 temperature steps (10^4 MC moves), resulting in four hot structures. The four hot configurations were then cooled separately on each of the four PESs from 300 to 1 K in 300 steps (10^5 MC moves), giving 16 cold BC_{12} structures.

The choice of 200 K as the upper temperature for smaller cluster simulations, though arbitrary, is reasonable. (1) In multiple test runs, optimized cluster structures were subjected to simulations at a temperature of 200 K over 2×10^6 MC steps. In every case, the final structure was fully randomized relative to the starting structure—confirming the melting temperature to be below 200 K. (2) A large collection of distinct final isomers is consistently generated from a single initial structure in all of these studies—empirically confirming that the 200 K structures are fully randomized. (3) Nothing substantial is lost even though the experimental clusters being compared were generated from a seeded mixture near 300 K. Warm structures at 200 K exist in a fluid form but undergo evaporation at significantly reduced rates relative to those at 300 K—consistent with our emphasis on cluster cooling after the evaporation process is essentially complete.

The four PESs used in the simulations were adapted for benzene−cyclohexane clusters from models developed by Williams,[23] van de Waal,[16] Shi and Bartell,[24] and Jorgensen[25].[22] Details of the four PESs are reproduced from ref 22 in edited form and included in the Appendix of this paper. All monomers are held rigid in these simulations. Benzene is assumed to possess D_{6h} symmetry, while cyclohexane is in the chair (D_{3d}) conformation. We carried out density functional theory optimization and frequency calculations (B3LYP/6-31g(d), frequency scaling factor = 0.9804) separately on the chair and boat conformations: The results reveal $\Delta G = 25.5$ kJ mol^{-1} for chair → boat isomerization at 298 K, equivalent to $>10RT$. At 0 K, the difference between the respective sums (electronic + zero point energy) is slightly larger: 27.1 kJ mol^{-1}. Although one might envision the possibility of one or more cyclohexane chair conformations rearranging to the boat form in exchange for improved intermolecular stabilization within the cluster, this appears unlikely. In the tetramer, for example (the largest BC_n cluster size with an identifiable number of major isomers), the transformation of only one chair → boat cyclohexane at 298 K would have to be compensated for by improvement of >45% in total cluster stabilization, without taking into account activation barriers.

The cluster coordinate system employed in the simulations assigns one opposing C−H bond pair in the benzene moiety as the cluster x-axis, with the cluster z-axis defined by benzene's molecular C_6 axis. The standard orientation of cyclohexane takes the molecular z-axis as its C_3 axis. The molecular $x-y$ plane is normal to the z-axis, with the origin defined by the molecular center of mass (CM). The x-axis is then defined by a ray connecting the CM to the projection of a carbon atom, having a positive z-coordinate, onto the $x-y$ plane. In the simulations, the benzene molecule is held fixed at the origin in its standard orientation. Each cyclohexane molecule is assigned six coordinates: Three (r, θ, ϕ) designate the CM in spherical polar coordinates, and the remaining three (α, β, γ), are Euler angles, identifying rotational orientation with respect to the standard cyclohexane orientation.

II.B. Symmetry Analysis and Isomer Identification. The newly formed cold structures were analyzed to identify unique structures (isomers). The configuration of each was evaluated against configurations of all of the remaining structures to test for symmetry equivalency.[22] $\langle(\Delta r)^2\rangle$ represents the mean-square difference in position and takes into account all carbon and hydrogen atomic coordinates in the structures being compared. Two structures are considered equivalent in this study when $\langle(\Delta r)^2\rangle$ is less than 0.30.[22] The units of $\langle(\Delta r)^2\rangle$ are square angstroms (Å^2) throughout this report.

II.C. Comparison to Model Structures. Part of the analysis involved a quantitative comparison of simulation results to model structures. The model structure for a given cluster size was defined as the corresponding minimum-energy configuration of a neat argon cluster. Specifically, model structures include: BC_3 = tetrahedron; BC_4 = trigonal bipyramid; BC_5 = octahedron; BC_6 = pentagonal bipyramid; BC_7 = hexagonal bipyramid; BC_{12} = icosahedron.[19]

Calculations assessed deviations between simulated and model structures, quantifying differences in both relative intermolecular distances and angles. In the model tetrahedron, for example, all molecular positions are equivalent, and distances between all pairs of molecules are equal. Molecular distances

in the Monte Carlo BC_3 structures were evaluated against those of a model tetrahedron, and a root-mean-square deviation was calculated. A parallel calculation assessed deviations between BC_3 intermolecular angles from those of a tetrahedron. It should be noted that molecular orientations were not considered in the deviation analysis, which was based solely on molecular center-of-mass positions; furthermore, distance deviation analysis was consistently based on ratios not absolute distances.

The model trigonal bipyramid contains three equatorial and two axial positions. To account for the two unique sites that can be occupied by C_6H_6 within a BC_4 cluster, two separate sets of molecule−molecule distance ratios were calculated for the model structure, each placing benzene in one of the two unique positions. Relative intermolecular distances of the Monte Carlo structures were then compared separately to axial and equatorial expectations. In addition, the intermolecular angle expectations of the model structure (axial, then equatorial) were compared to the simulated clusters, and root-mean-square differences were calculated.

An analogous strategy was adopted for larger BC_n clusters. With the exception of BC_5—for which the model octahedron has six equivalent sites—separate calculations assessed deviations from benzene in the axial versus equatorial positions of BC_6 and BC_7 and between C_6H_6 occupying the interior versus first-shell sites in BC_{12}.

II.D. Additional Studies on BC_3. Because the BC_3 simulations identified a finite number of well-defined isomers, additional studies were warranted.

II.D.1. Caloric Studies. For each of five major isomers, the mean cluster structure was heated separately on all four PESs from 1 to 200 K in 200 steps, each consisting of 5×10^4 MC steps. The first 2.5×10^4 steps were used to attain equilibrium at the new temperature; energies and positions were then monitored over the final 2.5×10^4 steps to determine average energy and standard deviations for (a) energy, (b) molecular centers of mass, and (c) atomic positions.

II.D.2. Isothermal Simulations at 5 K. Average isomer structures were run on the Shi PES at 5 K for 2×10^7 steps. The first 10^7 steps were applied to ensure equilibration; the final 10^7 steps were used to calculate thermally averaged cluster structures at 5 K. Resulting structures were compared quantitatively to standard (initial) structures to determine whether the initial isomer occupies a stable local minimum on the Shi PES at 5 K.

II.D.3. MP2 Optimization and Energy Calculations. The optimized structures and their corresponding electronic energies were calculated for two major MC isomers and also for one hypothetical isomer not identified by the MC simulations (next paragraph). These calculations used the 6-31g(d) basis set within the MP2 method and were run within the Gaussian 03W software suite.[26]

II.D.4. Analysis of Hypothetical Tetramer Structures. Three hypothetical structures—not identified by the simulations described in sections II.A−C—were constructed by combining the cyclohexane molecular coordinates of BC_1 on one side of benzene with those of the one-sided BC_2 Trigonal 3 Isomer (ref 22, in three different relative orientations) on the other side. The two-sided structures were optimized on each of the four PESs, and one was optimized via an MP2 electronic structure calculation. All three structures were analyzed as potential tetramer isomers, in the context of understanding and interpreting the R2PI experimental spectrum.

III. Results and Analysis

III.A. BC_3 Clusters. *III.A.1. Description of BC_3 Isomers.* From 80 independent simulations, five major BC_3 isomers were identified. Six minor isomers were also found. Major isomers are defined as those that were identified by at least 10% of the simulations; they also occupy a local minimum on all four PESs. Isomer 1 is subdivided because two PESs predict one optimized structure, and the other two PESs identify a very similar but slightly different optimized structure. Results from the Jorgensen and Shi PESs are referred to as Isomer 1A, and results from the Williams and van de Waal PESs are labeled Isomer 1B. Each of the four PESs predicts only one of the two structures, and the mean-square atomic displacement between the two is 0.30.

To define the mean structural coordinates for each isomer, optimized molecular coordinates (R, Θ, Φ, α, β, γ) from each PES were used to calculate Cartesian coordinates of all carbon and hydrogen atomic positions; the atomic coordinates were then averaged over the relevant PES structures, and the results were converted back to molecular coordinates via a nonlinear fit.

Because a large body of data was generated in this study, data tables that support but are not crucial to the narrative have been collected in the Supporting Information. Table numbers in the Supporting Information are preceded by the letter S. Tables S1−S6 list the mean molecular coordinates for all major BC_3 isomers, along with the optimized energy and the mean-square displacement of each individual PES structure relative to the mean structure. Mean structures resulting from the Monte Carlo studies are illustrated in Figures 1and 2. Figure 1 presents the isomers from the perspective of the $+z$-axis, while Figure 2 shows the same structures from the $+x$-axis.

III.A.1.a. BC_3 Isomer 1A. The mean structure for Isomer 1A is derived solely from the Jorgensen and Shi PES results. The molecular coordinates, minimum energy, and mean-square displacement values are listed in Table S1, and molecular stabilization energies for each PES are collected in Table S7. Documentation of the distribution of interaction stabilization energies specific to each PES is provided in Table S8**.** For Isomer 1A the total interaction energy is distributed among C_6H_6, C_6H_{12}-1, C_6H_{12}-2, and C_6H_{12}-3 in the approximate percentages 24%, 28%, 24%, and 24%, respectively. Individual molecular interaction energies are defined as one-half the sum of all atom−atom pair potential energies involving that molecule's atoms.

All three cyclohexane molecular centers of mass lie above the cluster $x-y$ plane (Figure 2). The cyclohexane molecule having its plane parallel to the plane of the benzene molecule is referred to as axial (Figure 2) and is represented by the C_6H_{12}-1 molecule in Isomers 1A, 1B, and 3 and is C_6H_{12}-3 in Isomer 5. For Isomer 1A the axial moiety is located 4.31 Å from the coordinate system origin with center of mass coordinates, (1.04, 0.01, 4.18) Å. The remaining two cyclohexanes, whose molecular planes cut the plane of the benzene moiety, are referred to as equatorial and are denoted as C_6H_{12}-2 and C_6H_{12}-3 for Isomers 1A, 1B, and 3. In Isomer 1A, their distances from the coordinate system origin are 5.70 and 5.50 Å, and their respective center of mass coordinates are (4.38, −3.20, 1.78) and (−0.51, −4.91, 2.41) Å. The axial molecule of Isomer 1A has a molecular tilt of 17.9° while the C_6H_{12}-2 and C_6H_{12}-3 equatorial molecules have molecular tilts of 71.2° and 75.0° respectively.

III.A.1.b. Isomer 1B. The mean structure of Isomer 1B is derived from the van de Waal and Williams PES results. Mean molecular coordinates, minimum energies, and mean-square

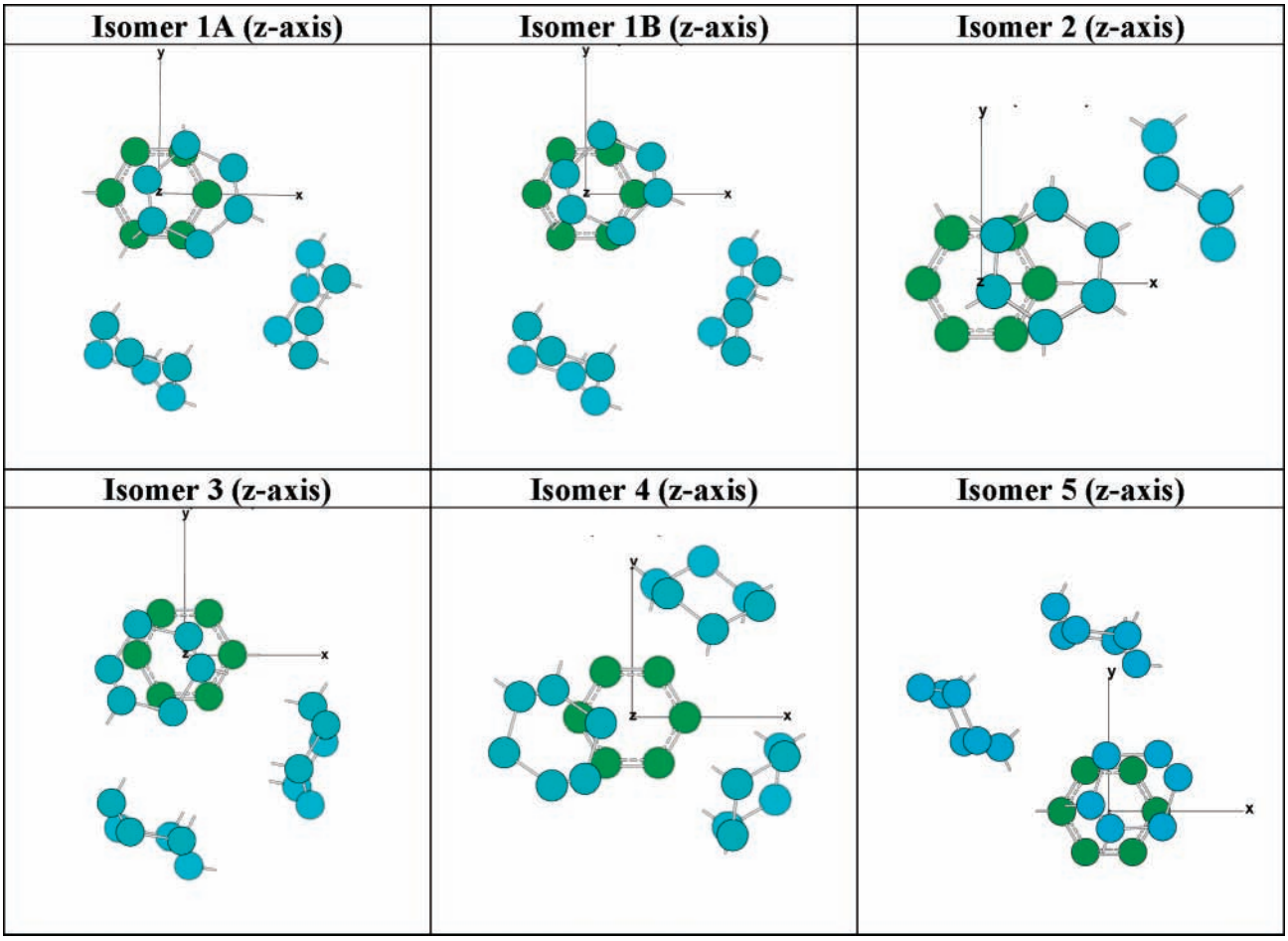

Figure 1. BC_3 isomers, viewed from the +*z*-axis. The carbon atoms in the benzene molecule are green, and the cyclohexane carbons are blue. Hydrogen atoms are not shown. Isomers 1A (Jorgensen and Shi) and 1B (Williams and van de Waal) are similar and are believed to represent a single isomer (see text).

displacement values are shown in Table S2. The total interaction energy is distributed among C_6H_6, C_6H_{12}-1, C_6H_{12}-2, and C_6H_{12}-3 in the approximate percentages 25%, 28%, 24%, and 23%, respectively. All cyclohexane molecular centers of mass lie above benzene's molecular plane (Figure 2). The axial cyclohexane is located 4.46 Å from the coordinate system origin with center of mass coordinates of (0.74, 0.30, 4.39) Å. Distances of the two equatorial molecules from the coordinate system origin are 5.86 and 5.67 Å, with corresponding center of mass coordinates of (4.41, −3.10, 2.30) and (−0.70, −4.88, 2.81) Å. The axial molecule of Isomer 1B has a molecular tilt of 27.7° while the C_6H_{12}-2 and C_6H_{12}-3 equatorial molecules have molecule tilts of 77.2° and 74.0°, respectively.

Direct comparison of Isomers 1A and 1B (Figures 1 and 2) reveals clear similarities. The molecular energy distribution of the two is the same within 1%. Differences between the center of mass coordinates in the two structures (in angstroms) are: C_6H_{12}-1, (0.30, −0.29, −0.21); C_6H_{12}-2, (−0.03, −0.10, −0.52); C_6H_{12}-3, (0.19, 0.03, −0.40); differences between absolute center of mass positions range from 0.44 to 0.53 Å. The difference between the axial molecule's molecular tilt is 9.8°, and the differences between the equatorial C_6H_{12}-2 and C_6H_{12}-3 tilts are 6.0° and 1.0°, respectively. Table 1 contains the mean-square coordinate differences of the cyclohexanes' 54 atomic coordinates, $\langle(\Delta r)^2\rangle$, evaluating coordinate differences between the five BC_3 isomeric structures. The mean-square displacement between Isomers 1A and 1B is small (<0.3) whereas the next smallest value between isomers is 0.86. Because of these similarities, we hypothesize that Isomers 1A and 1B are both approximations to the same "true" isomer.

III.A.1.c. Isomer 2. The mean structure of Isomer 2 is based on results from all four PESs. The molecular coordinates, minimum energies, and mean-square displacement values are listed in Table S3. The isomer's total interaction energy is distributed among C_6H_6, C_6H_{12}-1, C_6H_{12}-2, and C_6H_{12}-3 in the approximate percentages 32%, 21%, 21%, and 25%, respectively. Isomer 2 adopts the form of a modified "sandwich", with C_6H_{12}-1 and C_6H_{12}-2 on opposite sides of and nearly parallel to the plane of the benzene moiety (Figure 2). The sandwich structure distinguishes Isomer 2 from all other BC_3 isomers. The stacked structure results in more favorable interaction energy for the benzene moiety at the expense of cyclohexane−cyclohexane interactions—resulting in a net decrease in overall cluster stabilization. The two axial molecules are located 4.43 Å from the coordinate system origin and have center of mass coordinates, (1.60, 0.43, ±4.10) Å. Their molecular tilts are both 9.4°. The C_6H_{12}-3 center of mass is 5.46 Å from the origin; its center of mass lies in the cluster $x-y$ plane with coordinates (4.98, 2.24, 0.00) Å. The C_6H_{12}-3 molecular tilt is 90.0°. Quantitative analysis confirms that the structure of Isomer 2 is characterized by mirror symmetry, with reflection through the cluster $x-y$ plane yielding an equivalent structure.

III.A.I.d. Isomer 3. The Isomer 3 structure is based on results from all four PESs. The molecular coordinates, minimum energies, and mean-square displacement values are listed in Table S4. Isomer 3 is similar to Isomer 1 (A and B) in that the

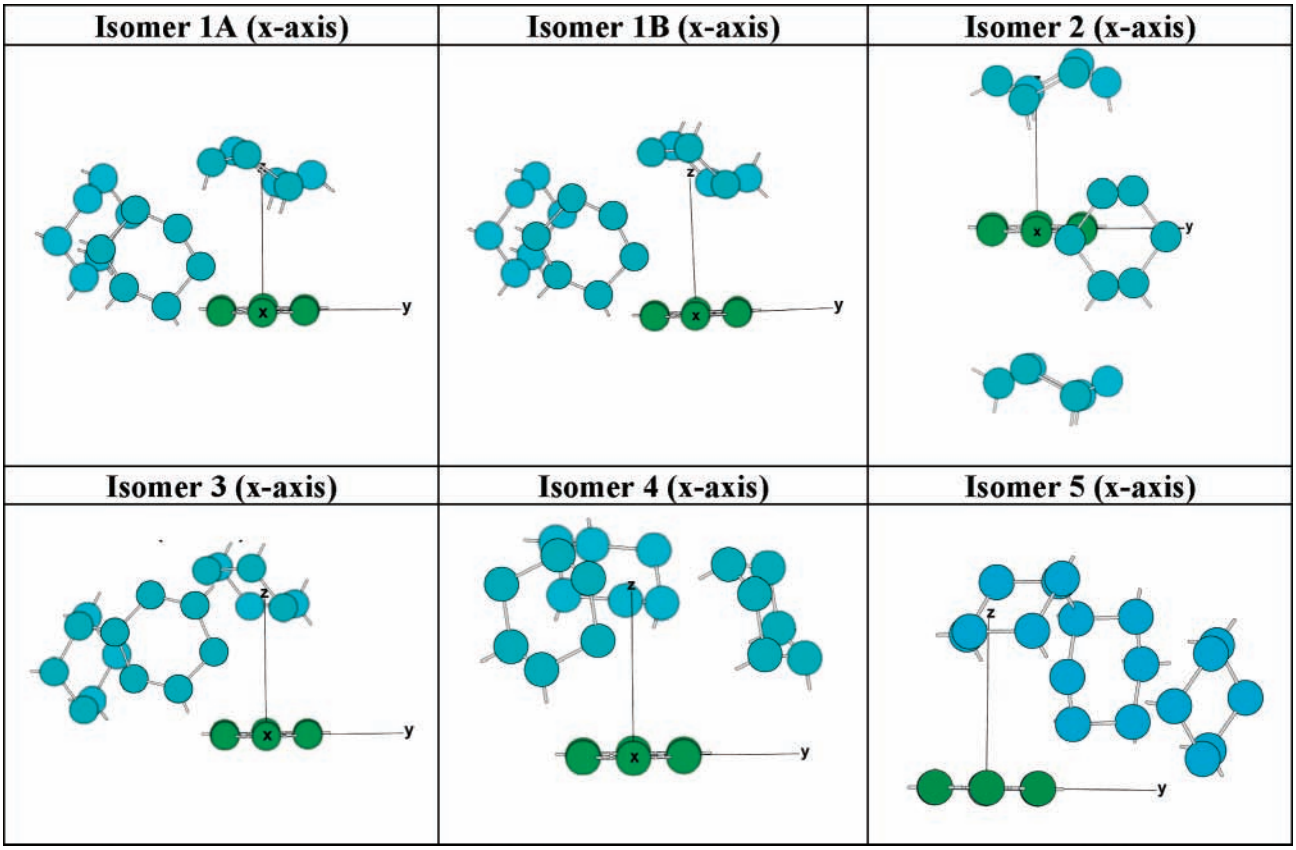

Figure 2. View of each BC_3 isomer from the $+x$-axis. The carbon atoms in the benzene molecule are green, and the cyclohexane carbons are blue. The hydrogen atoms are omitted. Isomers 1A (Jorgensen and Shi) and 1B (Williams and van de Waal) are similar and are believed to represent a single isomer (see text).

TABLE 1: Mean-Square Coordinate Differences, $\langle(\Delta r)^2\rangle$, of 54 Atomic Coordinates in the Three Cyclohexane Molecules, Comparing Structures of the Five Major BC_3 Isomers[a]

isomer	1B	2	3	4	5
1A	**[0.30]**	24	**2.6**	8.4	**1.1**
1B		27	**2.3**	6.7	**0.86**
2			27	37	26
3				6.7	**1.7**
4					9.0

[a] Units are Å^2. Isomers 1A and 1B (in brackets) are believed to represent the same isomer. Boldfaced entries indicate that the isomers are members of the same structural group, as identified in the text. All 11 (major and minor) isomers are compared in Table S55.

interaction energy is distributed among C_6H_6, C_6H_{12}-1, C_6H_{12}-2, and C_6H_{12}-3 in the approximate percentages 24%, 28%, 24%, and 24%, respectively, and that all three cyclohexane molecular centers of mass lie above the cluster $x-y$ plane (Figure 2). The axial cyclohexane molecule has a molecular tilt of 30.9° and is located 4.43 Å from the origin with center of mass coordinates, (−0.87, −0.40, 4.32) Å. The equatorial molecules are 5.57 and 5.75 Å from the origin, with respective center of mass coordinates of (3.72, −2.95, 2.91) and (−1.02, −5.25, 2.13) Å. These molecules have molecular tilts of 91.0° and 88.6°. In comparison to Isomer 1, the center of mass coordinates for all cyclohexanes in Isomer 3 differ by 0.07 to 2.0 Å. The differences between the C_6H_{12}-1, C_6H_{12}-2, and C_6H_{12}-3 molecular tilts when comparing Isomer 3 to Isomer 1 range from 3° to 13°, from 13° to 20°, and from 13° to 15°, respectively.

III.A.1.e. Isomer 4. The results for Isomer 4 are based on all four PESs. Molecular coordinates, minimum energies, and mean-square displacement values are documented in Table S5. For this isomer, the total interaction energy is distributed among C_6H_6, C_6H_{12}-1, C_6H_{12}-2, and C_6H_{12}-3 in the approximate percentages 25%, 24%, 26%, and 24%, respectively, with all four molecules benefiting nearly equally. Like Isomers 1 and 3, all of the cyclohexane molecular centers of mass lie on the same side of benzene's molecular plane. Isomer 4 is different, however, because it contains no axial cyclohexane (Figure 1). Locations of the C_6H_{12}-1, C_6H_{12}-2, and C_6H_{12}-3 molecules from the coordinate system origin are 5.23, 4.88, and 5.30 Å, respectively. The corresponding center of mass coordinates are (2.01, 3.25, 3.57), (−2.11, −0.54, 4.36), and (3.28, −7.98, 3.65) Å, respectively. The molecular tilt angles for C_6H_{12}-1, C_6H_{12}-2, and C_6H_{12}-3 are 64.1°, 144.5°, and 78.7°, respectively.

III.A.1.f. Isomer 5. The mean structure of Isomer 5 is based on all four PESs. The molecular coordinates, minimum energies, and mean-square displacement values are shown in Table S6. The isomer's interaction energy is distributed among C_6H_6, C_6H_{12}-1, C_6H_{12}-2, and C_6H_{12}-3 in the approximate percentages 24%, 24%, 25%, and 27%, respectively. Recalling that C_6H_{12}-3 is analogous to C_6H_{12}-1 in Isomers 1 and 3, the three distributions are similar. Like Isomers 1 and 3, Isomer 5 possesses an axial cyclohexane molecule, C_6H_{12}-3. (Table S13 and Figure 1). The distances of the C_6H_{12}-1, C_6H_{12}-2, and C_6H_{12}-3 molecules from the coordinate system origin are 5.23, 4.88, and 5.29 Å, respectively. The corresponding center of mass coordinates are (1.88, 3.03, 3.82), (−4.23, −1.06, 2.18), and (3.13, −1.90, 3.82) Å. The respective molecular tilts for C_6H_{12}-1, C_6H_{12}-2, and C_6H_{12}-3 molecules are 97.2°, 83.8°, and 33.9°.

III.A.1.g. Uniqueness of the Five Isomers. As discussed above, Isomers 1A and *1B* are hypothesized to represent the same isomer, based on similar molecular energy distributions, cyclohexane orientations, and a small mean-square displacement (0.3 Å^2) between the two. From Table 1, it is observed that

TABLE 2: Distinguishing Characteristics of the Three Structural Groups of BC_3[a]

group	cyclohexane location	no. axial	% of BC_3 clusters	average cluster *E* ratio (%)	average benzene *E* ratio (%)	average distance deviation (%)	average angle deviation (%)
1	all on same side of $x-y$ plane	1	77	99.7 (0.3)	83 (1)	10 (1)	15 (2)
2	all on same side of $x-y$ plane	0	12	98.9	86	5	5
3	both sides of $x-y$ plane	2	11	90.3	100	25	34

[a] Included are cyclohexane location, the number of axial molecules, percentage of BC_3 isomers represented by each group, average benzene and cluster energy ratios as defined in the text, and the average relative distance and angle deviations from the model tetrahedron, with standard deviations for Group 1 (in parentheses). Values are derived from the five major isomers.

Isomers 3 and 5 have the smallest mean-square displacement relative to Isomers 1A and 1B. For all three, all cyclohexane molecular centers of mass are located above the $x-y$ plane, one occupying an axial position with the other two being equatorial. Because absolute energies calculated for a given structure differ for each PES, energies were analyzed as ratios, relating the calculated energy to the most favorable energy (i.e., global minimum) value of all of the BC_3 isomers calculated on the same PES. The averaged energy ratios are used to directly compare results among the four PESs.

For Isomer 1A the mean ratio is 99.8% for the total cluster energy and 84.1% for the benzene stabilization energy. The benzene stabilization energy ratio, as used in this report, is defined as the benzene stabilization energy within the isomer, divided by the most favorable benzene stabilization energy among all same-sized isomers calculated on the same PES. The corresponding total-cluster and benzene stabilization energy ratios for Isomers 1B, 3, and 5 are (99.9%, 82.7%), (99.9%, 83.6%), and (99.4%, 81.7%) respectively. These values indicate that Isomers 1, 3, and 5 all have near-optimal overall cluster stabilization. Similarity between the three is confirmed by the mean-square atomic displacements, collected in Table 1.

Isomer 4 is different from Isomers 1, 3, and 5 because all cyclohexane centers of mass are located on the same side of the $x-y$ plane, but none occupies an axial position. The energy ratios for Isomer 4 are 98.9% for the total cluster energy and 86.3% for the benzene molecule stabilization energy. Like Isomers 1, 3, and 5, Isomer 4 has near optimal total cluster energy.

Isomer 2 is fundamentally different from the other four. This is demonstrated by its large mean-square displacement values (Table 1**)** relative to the other major isomers. This stems from Isomer 2 assuming a "sandwich" formation, containing two axial molecules and one equatorial, assembled with mirror plane symmetry. Energy ratios for Isomer 2 are 90.3% for the total cluster energy and 100% for the benzene stabilization energy. The sandwich configuration clearly maximizes benzene−cyclohexane interactions; however, this occurs at the expense of cyclohexane−cyclohexane interactions, with the net result being less favorable overall cluster stabilization.

III.A.2. Structural Groups in BC_3 Clusters. The Monte Carlo simulations attest to five well-defined major BC_3 isomeric structures and six minor isomers. These can be classified into groups; such classification establishes the foundation for discussing and analyzing BC_4 (and larger) clusters. As emphasized in the discussion that follows, all BC_n clusters, with $n \geq 4$, exist in a large number of isomeric forms, making the identification of individual isomer structures impractical for those sizes.

On the basis of the conclusion that Isomers 1A and 1B are representations of the same isomer, Isomer 1A was arbitrarily chosen to represent Isomer 1 in the following discussion. The 11 isomers of BC_3 clusters are conveniently classified into three structural groups.

III.A.2.a. BC_3 Group 1. Major isomers 1, 3, and 5 belong to Group 1 (Tables S1−S4 and Figures 1 and 2). Also in the group are minor isomers 6, 8, 9, and 10 (Tables S56, S58−S60, and S65 and Figures S1 and S2). For members of this group, all three cyclohexane moieties are located on the same side of the cluster $x-y$ plane. Furthermore, the cyclohexane molecules are positioned on the same half of the benzene hexagon (Figure 2) and therefore occupy only one quadrant of the coordinate system. The axial cyclohexane encircles the *z*-axis and is oriented horizontally, having a β (molecular tilt) coordinate <0.9 radians. Both equatorial cyclohexane molecules are vertically oriented ($\beta > 0.9$ radians). Of the 80 BC_3 simulations, 77% resulted in Group 1 structures.

III.A.2.b. BC_3 Group 2. Major isomer 4 and minor isomers 7 and 11 belong to Group 2 (Tables S5, S57, S61, and S65 and Figures 1, 2, S1, and S2). Like Group 1, Group 2 structures have all three cyclohexane molecules on the same side of the $x-y$ plane. However, they possess no axial cyclohexane molecule; instead, the three cyclohexane moieties form a triangular ring around the *z*-axis (Figure 1). Of the 80 BC_3 simulations, 12% resulted in Group 2 structures.

III.A.2.c. BC_3 Group 3. Isomer 2 is the sole member of Group 3 (Tables S3 and S65 and Figures 1 and 2), which is unique because of its mirror symmetry. All three cyclohexane molecules are on the same half of the benzene hexagon; two axial cyclohexanes are horizontally oriented ($\beta \approx 0.165$ radians) and stacked on either side of the $x-y$ plane (Figure 2). The equatorial cyclohexane is vertically oriented ($\beta = \pi/2$ radians) and is positioned in the cluster $x-y$ plane. Of the 80 BC_3 simulations, 11% resulted in Group 3 structures.

III.A.3. Energy and Deviation Comparisons for the BC_3 Structure Groups. Table 2 lists the average benzene stabilization energy and cluster energy ratios within each group of BC_3 isomers, with their standard deviations (in parentheses). Group 3 isomers have the most favorable benzene stabilization, while Group 1 has the least favorable. However, Group 3 has the least favorable overall cluster energy, and Group 1 has the most favorable. These observations reflect the fact that in BC_3 sandwich symmetry results in improved benzene−cyclohexane interactions at the expense of cyclohexane−cyclohexane interactions. Standard deviations of the benzene and total cluster energies within Group 1 (based on three major isomers) are small, providing additional justification of the group assignment. Values in Table 2 are derived from the five major isomers only.

To further assess the three groups, structures were quantitatively compared to expectations for a model tetrahedron, in which all intermolecular distances are equal and all A−B−C molecular angles are 60°. For each of the major isomeric structures, the average intermolecular distance was calculated, and the relative root-mean-square deviation (actual vs average distances) was determined (see average distance deviation in Table 2). Similarly, the 12 intermolecular angles within each isomeric structure were determined, and the relative root-mean-square difference from the tetrahedral model (60°) was calcu-

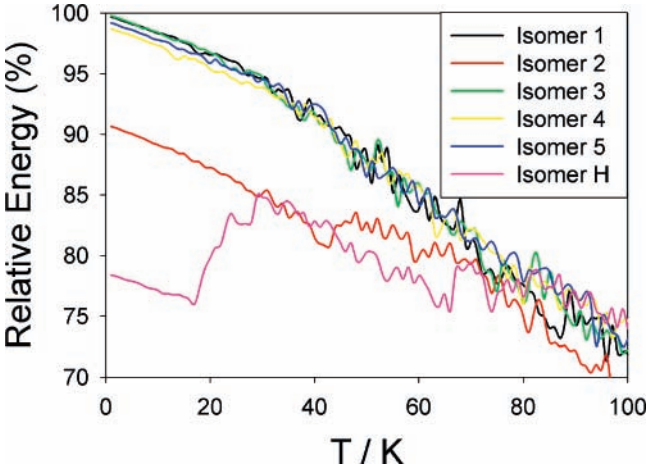

Figure 3. Relative mean energies of the five major BC_3 isomers and a hypothetical isomer (H) as a function of temperature from 1 to 100 K. Traces represent the average of independent runs on all four PESs at 1 K resolution. Energy data from each PES is first converted to relative energy (defined in the text) to allow for averaging.

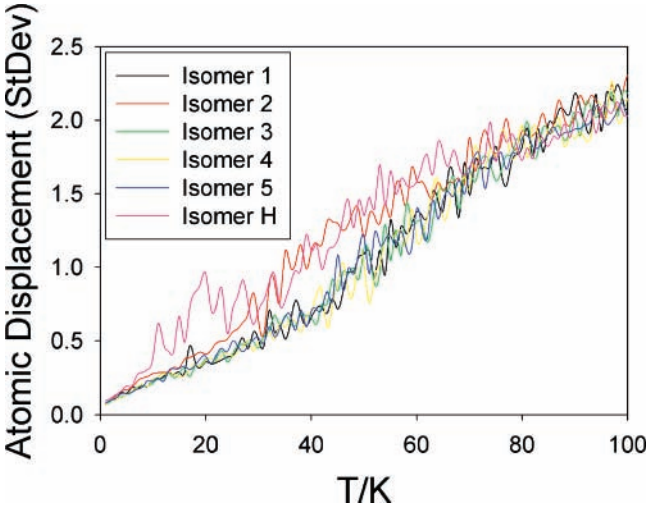

Figure 4. Mean atomic displacements, in angstroms, of the five major BC_3 isomers and one hypothetical isomer (H) when heated from 1 to 100 K. Traces represent the average of independent runs on all four PESs at 1 K resolution.

lated (average angle deviation). For Group 1 isomers, standard deviations in Table 2 are small. (For additional quantification, detailed distance and angle deviation data are collected in Table S14.) Group 2 structures show the smallest distance and angle deviations, conforming most closely to the model tetrahedron. Group 3 isomers have the largest deviations because the sandwich structure is significantly different from the model tetrahedron. Group 1 is intermediate but is much closer to the tetrahedral model than Group 3.

III.A.4. Summary of Characteristics of Structure Groups. Table 2 summarizes the defining characteristics of each group of BC_3 clusters. Group 1 has three cyclohexanes located above the $x-y$ plane with only one occupying an axial position. These isomers have the most favorable cluster energy values and the least favorable benzene energy values (Table 2). Group 1 isomers have intermediate distance and angle deviations from the model tetrahedral structure. Group 2 isomers also have all three cyclohexanes located on the same side of the $x-y$ plane; however, none of these occupies an axial position. They have favorable total cluster energies and are closest to the model tetrahedron (Table 2). In Group 3, two axial cyclohexane molecules are located on opposite sides of the $x-y$ plane, with an equatorial molecule in the plane. These structures have maximum benzene−cyclohexane interactions, accompanied by the least favorable total cluster energy (Table 2). They are significantly distorted from the tetrahedral model structure.

III.A.5. Caloric Studies. Figure 3 reveals the evolution in relative energy as each of the five major isomers and one hypothetical isomer are heated from 1 to 100 K. For each of the four PESs, the relative energy quantifies the temperature-dependent energy relative to the minimum optimized energy (i.e., *global minimum*) calculated among all tetramer isomers on the same PES. Traces represent the average value over all four PESs. Figure 4 shows the mean atomic displacements from average positions as a function of temperature, an indicator of molecular freedom of movement within the structure. The plots fail to distinguish Isomers 1, 3, 4, and 5. However, Isomer 2 and the hypothetical isomer H (described later) are each unique at temperatures below 25 K. Between 50 and 75 K, all of the isomers become indistinguishable. The uniqueness of isomers 2 and H—clearly demonstrated in Figures 3 and 4—is one important key to interpreting the experimental data (section IV.C).

III.A.6. Isothermal Simulations at 5 K. Because all 11 isomers occupy distinct local minima only on the Shi PES, isothermal simulations—starting with the minimum energy structures—were carried out on this PES to determine mean structures at 5 K. The results, documented in Table S66, indicate that minor Isomer 6 spontaneous rearranges to Isomer 3 at 5 K. This indicates a very low isomerization barrier between the two isomers. Three hypothetical isomers (described later) were also evaluated; only one of the three, H2, spontaneously isomerized to a different form, i.e., H1.

III.A.7. MP2 Optimization and Energy Calculations. Three separate MP2/6-31g(d) calculations were carried out using initial structures for Isomers 2, 3, and H2 as optimized on the Williams PES. The optimized MP2 coordinates are included in Tables S3, S4, and S63, and corresponding relative electronic energies are determined to be 0, +0.5, and +4.4 kJ mol^{-1}, respectively. MP2-optimized structures are close, though not identical to the MC structures, with $\langle(\Delta r)^2\rangle$ values ranging between 1 and 3 $Å^2$ relative to the corresponding mean MC structures.

III.B. BC_4 Clusters. In BC_4 and all larger BC_n clusters, a minimum of 14 isomers were identified for each cluster size. In all cases, the isomer count was limited by the number of simulations, and the existence of additional unidentified isomers is certain. As a result, a detailed description of individual isomer structures for BC_n ($n \geq 4$) is impossible. Nevertheless, the situation is not hopeless because structures are observed to fall into identifiable groups. The characterization and description of these structural groups provides useful insight into general properties, intermolecular interactions, and structural relationships between neighboring-size clusters.

III.B.1. BC_4 Structural Groups. Twenty-eight simulations (7 on each PES) identified 23 unique structures, establishing a lower limit for the number of BC_4 isomers. No attempt was made to identify each isomer on all four PESs to obtain an average structure; therefore, the molecular coordinates represented in Tables S15−S18 are specific to the PES on which the simulation was run. It is observed that BC_4 structures can be classified into two major groups, each consisting of two subgroups. Representations of the subgroups are presented in Figure 5, wherein each structure is shown from two different perspectives in the $x-y$ plane.

III.B.1.a. BC_4 Group 1. In Group 1 structures, cyclohexane molecules are both above and below the $x-y$ plane but are

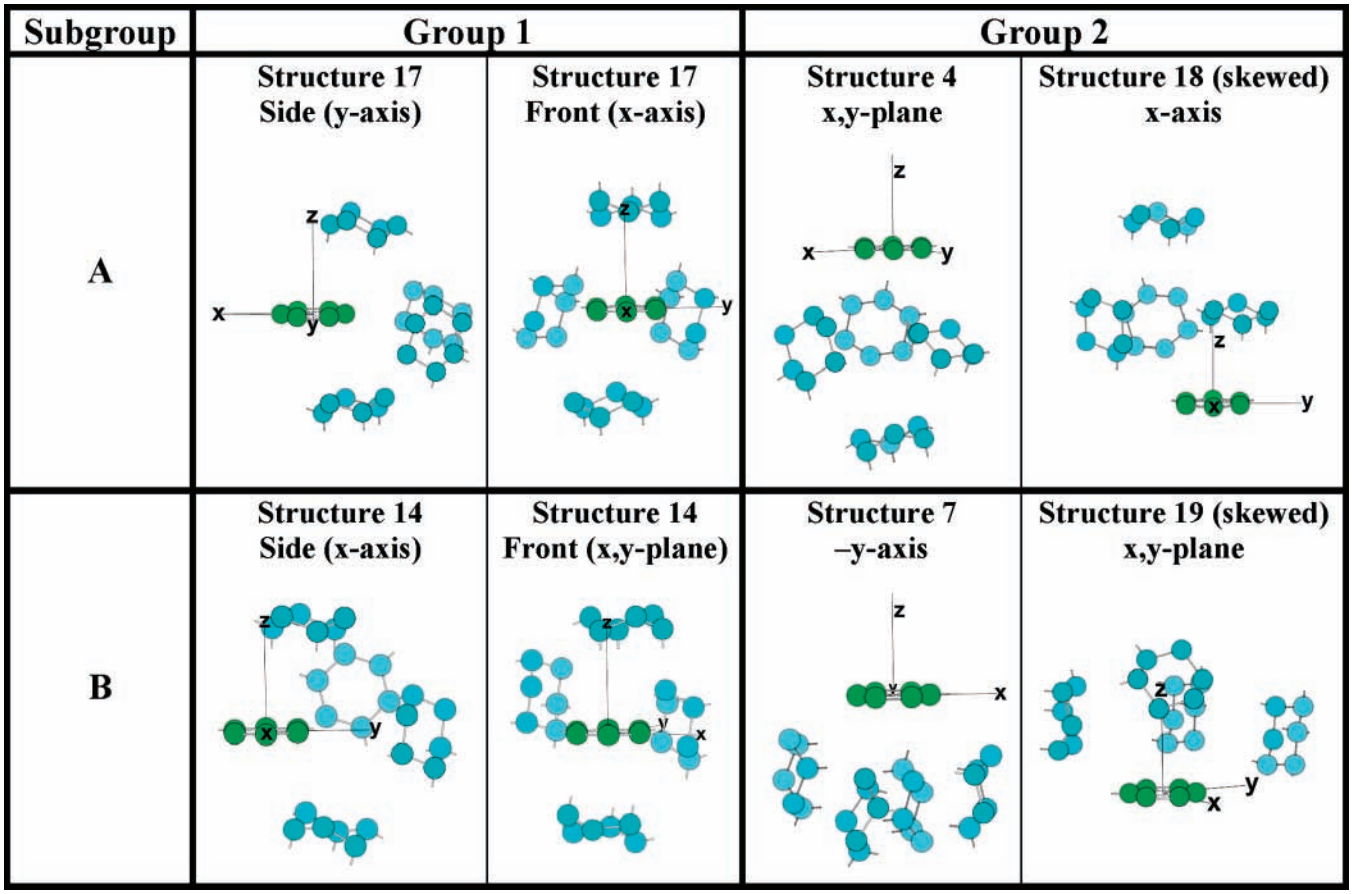

Figure 5. Representative structures for each structural subgroup of BC_4 clusters. Structures are shown from two different views in the $x-y$ plane. The carbon atoms in the cyclohexane molecules are blue, and the carbon atoms in the benzene molecule are green. Hydrogen atoms are not shown for clarity.

confined to one-half of the benzene hexagon. The cyclohexane molecules form a partial shell around the benzene (Figure 5). Each Group 1 structure has two cap molecules, i.e., cyclohexane moieties located on either side of the $x-y$ plane with centers of mass near the z-axis. The cap molecules are generally horizontal in orientation, having small β (molecular tilt) coordinates; they are not, however, precisely parallel to each other. The remaining two cyclohexane molecules form the midsection of a half shell.

Table S15 lists the molecular coordinates for isomers identified with subgroup 1A. In these structures three cyclohexane centers of mass (CMs) are located on one side of the benzene plane and one on the other (Figure 5; structure 17). The two noncap cyclohexane molecules tend to be oriented more vertically than horizontally, and—because they are on the same side of the $x-y$ plane—both are closer to the same cap molecule than to the other. The molecular coordinates of structures identified with subgroup 1B are listed in Table S16. Structures in subgroup 1B have the cyclohexane CMs evenly split on either side of the $x-y$ plane; this is the only structural distinction between subgroups 1A and 1B. Fifteen of 23 BC_4 simulation structures (∼65%) belong to Group 1. Of these, 12 are in subgroup 1A, and three in subgroup 1B, corresponding to ∼52% and ∼13% of the BC_4 population.

III.B.1.b. BC_4 Group 2. All four cyclohexane molecules in the isomers identified with Group 2 are located on the same side of the $x-y$ plane. Group 2 is subdivided (2A and 2B) on the basis of cyclohexane positions and orientations. Molecular coordinates for subgroup 2A structures are listed in Table S17, and those corresponding to subgroup 2B are in Table S18. In subgroup 2A, a ring consisting of three cyclohexanes is observed, with the benzene moiety oriented horizontally on one side of the ring and a cyclohexane oriented horizontally on the opposite side (Figure 5). In some subgroup 2A structures, the ring is not centered about the cluster z-axis. Furthermore, the molecules above and below the triangular ring are not exactly parallel to each other. The distinguishing feature of subgroup 2A is the presence of a three-member cyclohexane ring. In the structures belonging to subgroup 2B all four cyclohexane moieties assume a relatively vertical orientation and form a staggered ring either above or below the benzene molecule (Figure 4). The four-member ring need not be centered about the z-axis, nor are the four centers of mass exactly coplanar. Eight of the 23 BC_4 structures (∼35%) belong to Group 2. Of these, six are in subgroup 2A, and the remaining two are in 2B. Of the BC_4 population, these represent ∼26% and ∼9%, respectively.

III.B.2. Energy and Deviation comparisons for BC_4. Because simulations were run on four different PESs, computed energies cannot be compared directly. Instead, the ratios of a given structure's benzene stabilization energy and total cluster energy, relative to the most favorable benzene and total cluster energies among all of the isomers calculated on the same PES, were used for comparison. Table 3 lists the average benzene and cluster energy ratios for each BC_4 structural subgroup, along with their associated standard deviations. Complete documentation of the benzene and total cluster energy ratios for all structures is collected in Table S19. Total energy ratios average from 95% to 100% for all subgroups. Nevertheless, a clear distinction between groups is observed in the benzene molecule's stabilization energy. Subgroups 1A and 1B both have large benzene energy ratios, i.e., from 97% to 100% of the corresponding optimal benzene stabilization. Subgroups 2A and

TABLE 3: Average Benzene Energy Ratio and Cluster Energy Ratio along with Their Corresponding Standard Deviations (in Parentheses) for Each BC_4 Subgroup[a]

properties	Group 1A	Group 1B	Group 2A	Group 2B
average benzene *E* ratio (%)	98.2 (2.2)	97.0 (0.9)	71.3 (3.9)	86.0 (0.9)
average cluster *E* ratio (%)	98.9 (0.9)	99.7 (0.4)	99.2 (0.5)	95.9 (1.3)
average distance deviation (%)	8.5 (1.4)	9.1 (0.6)	9.5 (4.7)	8.9 (0.4)
axial	17.0 (1.1)	17.5 (0.5)	7.4 (2.4)	18.3 (0.1)
equatorial	11.0 (1.5)	11.5 (0.9)	22.3 (1.7)	6.4 (5.9)
average angle deviation (%)	13.7 (1.8)	14.7 (1.3)	13.7 (3.4)	13.5 (1.9)
axial	20.2 (1.8)	19.6 (1.2)	14.2 (2.7)	21.5 (4.3)
equatorial	12.8 (2.2)	13.5 (1.2)	20.4 (1.1)	12.6 (4.2)

[a] Also included are the distance and angle deviations, analyzing for benzene in the axial and equatorial positions of a trigonal bipyramid. All values are in percent.

2B have smaller ratios, ranging from 70% to 86%, reflecting decreased benzene−cyclohexane, but increased cyclohexane−cyclohexane interactions. Also included in Table 3 are the average distance and angle deviations from the model trigonal bipyramid. All two-molecule interaction distances are considered, as are all three-molecule angles. In addition, analysis of benzene's position (axial versus equatorial) within the model was undertaken. (For detailed documentation of the results for each of the 23 BC_4 structures, see Table S20.) From Table 3, it is observed that all subgroups of BC_4 clusters have similar overall distance (8.5−9.5%) and angle (13.5−14.7%) deviations from the trigonal bipyramid. A distinction between subgroups is seen in the axial versus equatorial analysis. In Figure 6, a representative structure from each subgroup of BC_4 is shown to emphasize the benzene molecule's position (axial or equatorial). In subgroups 1A, 1B, and 2B, benzene more closely occupies an equatorial position, based on both the distance and angle deviations and confirmed by studying the structures. Subgroup 2A is unique in that its benzene occupies an axial position.

III.B.3. Summary of Characteristics of Structure Subgroups. Table 4 summarizes the defining characteristics of each BC_4 subgroup. Subgroup 1A and 1B structures have a partial-shell cyclohexane formation with benzene in an equatorial position, resulting in favorable benzene stabilization energies. Subgroup 1A structures have three cyclohexane CMs located above the $x-y$ plane while subgroup 1B structures only have two. Respectively, the subgroups account for ∼52% and ∼13% of the total BC_4 population. Subgroup 2A and 2B structures have all four cyclohexane molecules located on the same side of the $x-y$ plane and exhibit the least favorable benzene stabilization energies. In subgroup 2A, three cyclohexanes form a triangular ring, and benzene occupies an axial position. In subgroup 2B all cyclohexanes combine to form a four-member ring, and benzene occupies an equatorial position. Of all simulated BC_4 structures, subgroups 2A and 2B account for ∼26% and ∼9%, respectively.

III.C. BC_5 Clusters. From 28 simulations, 26 unique BC_5 isomers were identified. The molecular coordinates of each isomer are documented in Tables S21−S28. BC_5 isomers were classified into three major groups. Representative structures from each subgroup in Groups 1 and 2 are illustrated in Figure 7, and Group 3 subgroups are represented in Figure S4. Detailed analysis of the BC_5 subgroups—including their structures and energies (analogous to sections III.B.1−2 for BC_4)—is included in the Supporting Information; only a summary of that analysis is included here.

Table 5 summarizes the key characteristics of each BC_5 subgroup. The structures belonging to subgroups 1A, 1B, and 1C all have a partial shell formation around the benzene molecule, lack a four molecule plane, and possess relatively high benzene stabilization energy ratios—with the exception of subgroup 1C, whose benzene stabilization is only moderate. The structures of subgroup 1A have two vertically oriented cyclohexanes located in the $x-y$ plane, while subgroup 1B has only one. Subgroup 1C also has one cyclohexane located in the $x-y$ plane, but it assumes a horizontal orientation. The percentage of BC_5 clusters possessing the characteristics of subgroups 1A, 1B, and 1C are ∼19%, ∼19%, and ∼4%, respectively. Group 2 structures lack a four molecule plane and possess four cyclohexanes located on the same side of the $x-y$ plane, three of which form a triangular ring. These structures have moderate benzene stabilization energy ratios and represent ∼12% of all BC_5 clusters. Subgroups 3A, 3B, 3C, and 3D all possess a quasi-four-molecule plane, with true planarity decreasing in the order 3A > 3B > 3C > 3D. Cyclohexanes in 3A are located on both sides of the $x-y$ plane forming a partial shell around the benzene; in subgroups 3B, 3C, and 3D the cyclohexanes are all located on the same side of the $x-y$ plane and form the four-member ring structure. Furthermore, 3A has relatively large benzene stabilization; in contrast, the corresponding ratio for 3B, 3C, and 3D is relatively small. The percentages of BC_5 clusters belonging to subgroups 3A, 3B, 3C, and 3D are ∼4%, ∼23%, ∼8%, and ∼12%, respectively.

III.D. BC_6 Clusters. All 28 structures obtained from the BC_6 simulations represent unique isomers. Molecular coordinates for individual isomers are tabulated in Tables S31−S40. BC_6 clusters were classified in four groups, and representative structures are presented in Figures S5−S8. All BC_6 structures were evaluated in terms of conformity to the model pentagonal bipyramid (PBP) structure. As part of the analysis, a three-dimensional (3-D) linear regression to the equation of a plane was performed using the CM coordinates of the five molecules appearing to be most closely coplanar. Resulting average R^2 values, listed in Table S69 for each subgroup, and the results from the deviation calculations were primary considerations in the classification of BC_6 structures. The relative deviations for (a) cluster CM-to-molecule distances, (b) molecule-to-molecule distances, and (c) axial versus equatorial angles for each subgroup are collected in Table S70. Detailed results of the deviation analysis for individual isomers are collected in Table S41. Detailed analysis of the BC_6 subgroups—including their structures and energies (analogous to sections III.B.1−2 for BC_4)—is included in the Supporting Information; only a summary of that analysis is included here.

Table 6 summarizes key characteristics that distinguish the BC_6 subgroups. As the group number increases, the balance between the number of cyclohexane molecules above/below the benzene plane becomes more lopsided. In general, the more uneven the cyclohexane distribution, the less effectively the benzene molecule is stabilized. Subgroups 1A, 1B, 2A, 3A, 4A, and 4B have PBP-like structures, based on the presence of a five-molecule plane and/or small distance and angle deviations relative to the model PBP. These represent 60% of the subgroups; however, they represent a smaller fraction (30%) of the 28 simulated BC_6 structures.

III.E. BC_7 Clusters. A total of 14 simulations were carried out on BC_7 clusters, all using the Jorgenson PES. (The choice of the Jorgensen PES was arbitrary for the BC_7 simulations.) Molecular coordinates for the 14 structures, all unique, are listed

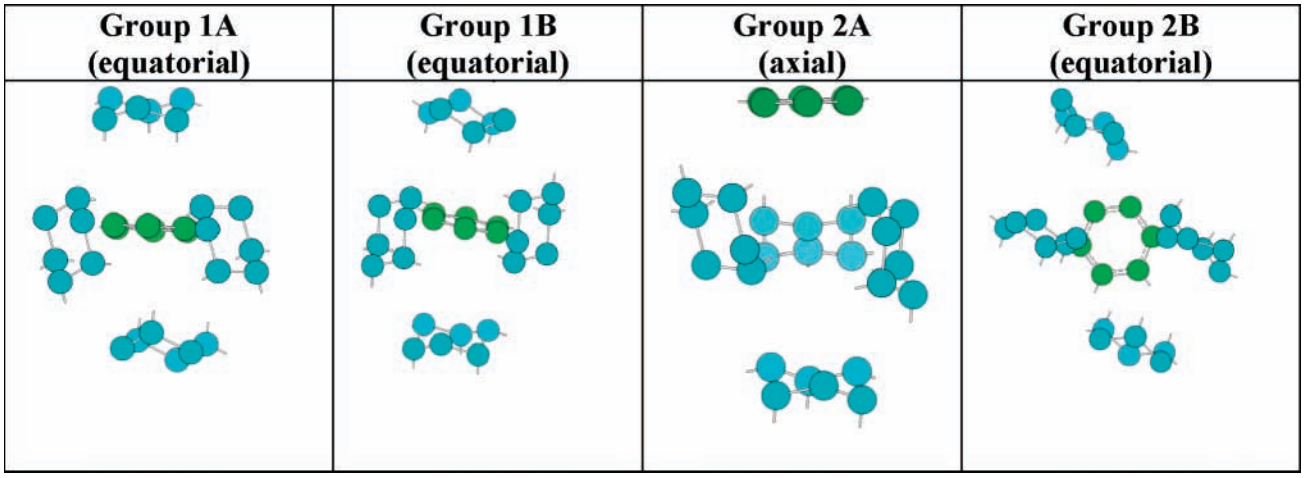

Figure 6. Each BC_4 subgroup is illustrated to emphasize the position of the benzene molecule (axial or equatorial). Carbon atoms in cyclohexane, are blue and those in benzene are green.

TABLE 4: Key Characteristics of the Four BC_4 Subgroups, Including Cyclohexane Location and Formation, Fraction of Clusters Represented, Average Benzene Energy Ratio, and Benzene Position within a Quasi-Trigonal Bipyramid

subgroup	cyclohexane location	cyclohexane formation	percentage of BC_4 clusters (%)	average benzene *E* ratio (%)	axial or equatorial benzene
1A	3 above *x*−*y* plane 1 below	partial shell	52	98.2	equatorial
1B	2 above *x*−*y* plane 2 below	partial shell	13	97.0	equatorial
2A	all above *x*−*y* plane	three-member ring	26	71.3	axial
2B	all above *x*−*y* plane	four-member ring	9	86.0	equatorial

in Tables S43−S45. Representative structures of the two BC_7 structural groups are illustrated in Figure S9.

Our analysis included a 3-D linear regression to the equation of a plane, using the six most coplanar cluster members. The largest calculated R^2 value was 0.225, indicating that none of the BC_7 structures closely resembles a hexagonal bipyramid. The distance deviation calculations (Tables S47 and S71) further confirm the lack of conformity to the model structure. Detailed analysis of the BC_7 subgroups—including their structures and energies (analogous to sections III.B.1−2 for BC_4)—is included in the Supporting Information; only a summary of that analysis is included here.

Table 7 summarizes the characteristics of the BC_7 subgroups. Group 1 structures contain cyclohexanes located on both sides of the *x*−*y* plane and have relatively high benzene stabilization energy ratios. Cyclohexanes in subgroup 1A are restricted to one-half of the benzene hexagon, whereas one of the cap molecules crosses the *z*-axis in subgroup 1B. The majority of the cyclohexane molecules in Group 2 are located on the same side of the *x*−*y* plane and are restricted to a single quadrant of the benzene hexagon. Group 2 structures have relatively low benzene stabilization ratios. Respectively, subgroups 1A, 1B, and 2 represent ∼79%, ∼7%, and ∼14% of the BC_7 population.

III.F. BC_{12} Clusters. A total of 20 calculations were run for BC_{12}, five on each of the four PESs. All 20 structures are unique. Molecular coordinates of the 20 structures are collected in Tables S48−S53. BC_{12} clusters were divided into six groups based on degree of conformity to the model icosahedron. Distance and angle deviations for the BC_{12} structural groups are tabulated in Table S72, and detailed data for individual structures are included in Table S54. Representative structures of the BC_{12} groups are shown in Figure S10. Six (30%) of the structures are compact, with benzene surrounded by a complete cyclohexane shell (Table S72); in contrast, no closed-shell structure is observed with a cyclohexane molecule occupying the interior position. All BC_{12} structures are related to the closed-shell structure, differing primarily by the number of cyclohexane molecules displaced from the first-shell positions; all BC_{12} structures have the benzene molecule in or near the cluster center, surrounded by a complete or partial shell of cyclohexane molecules (Figure S10). Detailed analysis of the BC_{12} subgroups—including their structures and energies (analogous to sections III.B.1−2 for BC_4)—is included in the Supporting Information; only a summary of that analysis is included here.

Table S74 summarizes distinguishing characteristics of the BC_{12} groups. Group 1 structures, representing 30% of the simulated structures, are characterized by a quasi-icosahedral 12-member cyclohexane shell surrounding benzene in the cluster interior. As the group number increases by one, one cyclohexane molecule is removed from the first solvation shell, resulting in a less icosahedron-like structure.

IV. Discussion

IV.A. Number of Isomers as a Function of Cluster Size. The isomeric structures of BC_1 and BC_2 were identified and characterized in a previous report.[22] BC_1 is represented by a single isomer possessing a parallel-displaced structure. Eight BC_2 isomers were reported: Three assume parallel-stacked (sandwich) structures, and five have trigonal arrangements.[22] The present study establishes the coexistence of five major BC_3 isomers and as many as six minor isomers. One isomer assumes a mirror-symmetry, modified sandwich arrangement, but the others lack overall symmetry. For cluster sizes larger than BC_3, our Monte Carlo simulations reveal a plethora of isomers, making the identification and characterization of individual isomers impossible. For BC_n, the tetramer (BC_3) is the largest cluster size having a manageable number of identifiable structural isomers.

IV.B.Evolution of Structure as a Function of Cluster Size. *IV.B.1. Relationships between BC_n and BC_{n+1} Structures for n = 1−6:* IV.B.1.a. BC_1 and BC_2. The three "sandwich" isomers of BC_2 are directly related to the parallel displaced BC_1 isomer by the addition of one cyclohexane moiety on the opposite side

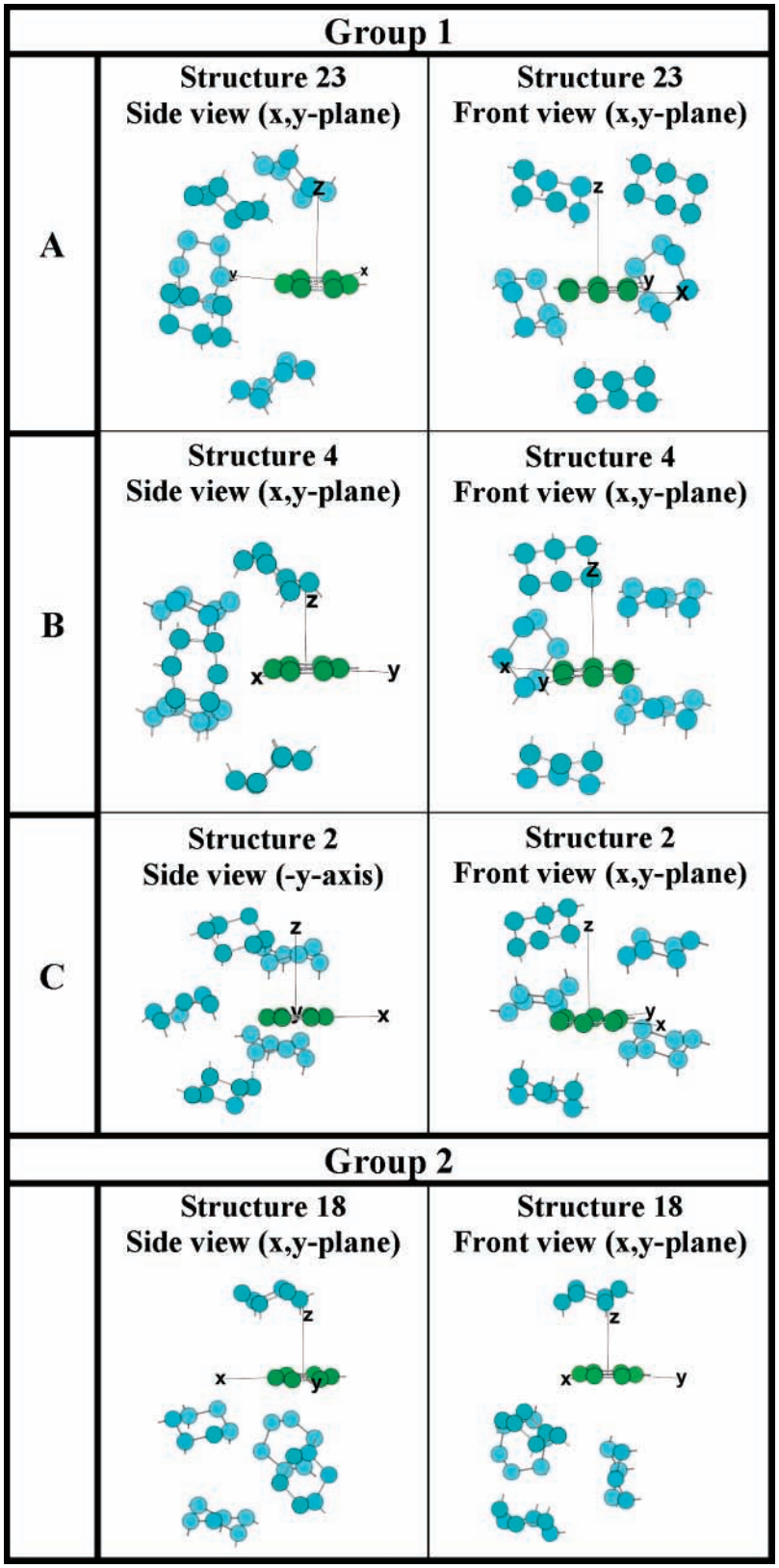

Figure 7. Representative structures for BC_5 Groups 1 and 2. Structures are shown from two different views in the $x-y$ plane. Cyclohexane carbon molecules are blue, and those of benzene are green. Hydrogen atoms are omitted. Detailed analysis of BC_5 groups is included in the Supporting Information.

of the benzene molecule. Of the eight BC_2 isomers, three share this direct relationship to the BC_1 structure.[22]

IV.B.1.b. BC_2 and BC_3. Three general relationships are observed between BC_2 and BC_3 clusters. First, the modified BC_3 sandwich isomer (Isomer 2 in Figures 1 and 2) has two parallel axial cyclohexanes, mutually related by reflection through the $x-y$ plane—identical to the BC_2 Sandwich 2 isomer and similar to Sandwiches 1 and 3.[22] Second, the Trigonal 1, 4, and 5 isomers of BC_2 are related to BC_3 Group 1 (which contains isomers 1A, 1B, 3, and 5; Figures 1 and 2) in that both groups contain one axial and one or more equatorial cyclohexanes. Finally, the BC_2 Trigonal 2 and 3 isomers both

TABLE 5: Key Characteristics of the Subgroups of BC_5 Clusters Including Cyclohexane Location, Cyclohexane Formation, and the Regression Coefficient (R^2) from the Linear Plane Fit[a]

subgroup	cyclohexane location	cyclohexane formation	four molecule plane/R^2 range	percentage of BC_5 clusters (%)	average benzene *E* ratio (%)
1A	2 in plane, 2 above, 1 below $x-y$ plane	partial shell	no four molecule plane	19	96.8
1B	1 in plane (vertical), 2 on either side of $x-y$ plane	partial shell	no four molecule plane	19	97.8
1C	1 in plane (horizontal), 2 on either side of $x-y$ plane	partial shell	no four molecule plane	4	80.4
2	1 above and 4 below $x-y$ plane	three-member ring	no four molecule plane	12	81.3
3A	1 in plane (vertical), 2 on either side of $x-y$ plane	partial shell	four molecule plane/$R^2 = 0.933$	4	95.7
3B	all above $x-y$ plane	four-member Ring	four molecule plane/$0.79 < R^2 < 0.89$	23	68.0
3C	all above $x-y$ plane	four-member ring	four molecule plane/ $0.60 < R^2 < 0.70$	8	68.8
3D	all above $x-y$ plane	four-member Ring	four molecule plane/ $0.40 < R^2 < 0.50$	12	65.0

[a] Also included are the percent of BC_5 structures assigned to each group and average benzene stabilization ratios.

TABLE 6: Key Characteristics of the Subgroups of BC_6 Clusters Including Cyclohexane Location, Cyclohexane Formation, Presence of a Five-Molecule Plane, Benzene Position (Axial/Equatorial), Percent of Simulated Structures Representing the Group, and the Benzene Molecule Stabilization Ratio

subgroup	cyclohexane location (relative to $x-y$ plane)	cyclohexane formation	five molecule plane	average deviations (%)	axial or equatorial benzene	percentage of BC_5 clusters (%)	average benzene *E* ratio (%)
1A	3 above and 3 below	partial shell	moderate fit	small	axial	7	91.4
1B	3 above and 3 below	partial shell	five molecule plane	large	equatorial	7	97.8
1C	3 above and 3 below	partial shell	none	large	N/A	25	94.1
2A	2 on one side and 4 on the other	partial shell	moderate fit	small	axial	4	97.6
2B	2 on one side and 4 on the other	three-member ring	none	large	N/A	18	80.8
3A	1 on one side and 5 on the other	partial shell	five molecule plane	large	equatorial	4	63.6
3B	1 on one side and 5 on the other	partial shell encircles *z*-axis	moderate fit	large	N/A	11	67.9
4A	6 on one side	encircles *z*-axis	none	small	axial	4	65.2
4B	6 on one side	encircles *z*-axis	five molecule plane	large	equatorial	4	64.8
4C	6 on one side	encircles *z*-axis	none	large	N/A	18	62.7

TABLE 7: Key Characteristics of the BC_7 Subgroups: Cyclohexane Location, Percentage of BC_7 Clusters Belonging to the Subgroup, and the Benzene Energy Ratio

subgroup	cyclohexane relative to $x-y$ plane	cyclohexane relative to *z*-axis	percentage of BC_4 clusters (%)	average benzene *E* ratio (%)
1A	both sides of $x-y$ plane	one side of benzene hexagon	79	90.8
1B	both sides of $x-y$ plane	both sides of benzene hexagon	7	99.6
2	6 or 7 on one side of $x-y$ plane	one quadrant of benzene hexagon	14	49.3

have cyclohexane moieties positioned well above the $x-y$ plane, similar to BC_3 Group 2 (containing isomer 4; see Figures 1 and 2). Structural connections between BC_n and BC_{n+1} subgroups are indicated in Figure 8.

IV.B.1.c. BC_3 and BC_4. BC_4 structures can be related to BC_3 by the addition of a cyclohexane molecule in one of the following three ways. First, BC_4 Group 1 (A or B; Figure 5) can be formed by the addition of an axial C_6H_{12} to BC_3 Group 1 (Isomers 1A, 1B, 3, and 5; Figures 1 and 2) or by the addition of an equatorial molecule to Group 3 (Isomer 2; Figures 1 and 2). Second, BC_4 Group 2A structures (Figure 5) are related to BC_3 Group 2 (Isomer 4; Figures 1 and 2) via the addition of a cyclohexane on the side of the trigonal cyclohexane ring that is opposite the benzene molecule. Finally, BC_4 Group 2B structures can be constructed by addition of one cyclohexane either to BC_3 Group 1 or to Group 2 structures.

IV.B.1.d. BC_4 and BC_5. Inspection of Figures 5, 7, and S4 reveals two general relationships between BC_4 and BC_5 structures. BC_5 Group 1, Group 2, and Group 3A structure types can all be created by the addition of one cyclohexane to BC_4 Group 1. BC_5 subgroups 3B, 3C, and 3D structures can be generated by the addition of one C_6H_{12} to a BC_4 Group 2 structure.

IV.B.1.e. BC_5 and BC_6. Comparison of Figures 7 and S4 with Figures S5−S8 reveals two general relationships between the two cluster sizes. BC_6 Group 1 and Group 2 structures can be generated by addition of a cyclohexane molecule to a BC_5 Group 1, 2, or 3A structure. Similarly, Groups 3 and 4 structures can be derived by addition to a BC_5 subgroup 3B, 3C, or 3D isomer.

IV.B.1.f. BC_6 and BC_7. The BC_7 Group 1 structures can be constructed by addition to a BC_6 Group 1 or Group 2 structure. Similarly, BC_7 Group 2 structures can be attained by adding to a BC_6 Group 3 or Group 4 isomer.

Figure 8 summarizes general structural connections between adjacent-sized cluster groups. Solid lines connect BC_n to BC_{n+1} groups whose structures are most similar. It is important to emphasize that in nearly all cases, addition of one cyclohexane molecule to BC_n, by itself, is insufficient to generate the related structure of BC_{n+1}; the addition must be accompanied by repositioning and reorientation of the original BC_n member molecules. The relationships are important because they predict major paths that will be followed if a BC_{n+1} cluster is built via addition to a rigid BC_n cluster or, conversely, if a BC_n cluster results from rigid-BC_{n+1} evaporation. Two evolutionary tracks are observed in Figure 8. The left track contains structures that maximize cyclohexane−cyclohexane interactions and tend to exclude the benzene moiety from the cluster center. In contrast, structures in the right track tend to place benzene in or near the cluster center, maximizing the benzene molecule's stabilization via solute−solvent interactions. The two tracks are generally isolated but are connected between BC_3 and BC_4.

IV.B.2. Fraction of Clusters Similar to the Model Structures. BC_2 clusters with a trigonal arrangement are most similar to the model structure, an equilateral triangle. Five of the eight BC_2 isomers (62.5%) have a trigonal structure.[22] The BC_3 isomers in Group 2 most closely resemble a tetrahedron, and those in Group 1 have structures that are somewhat tetrahedral: These represent 12% and 77% of calculated structures,

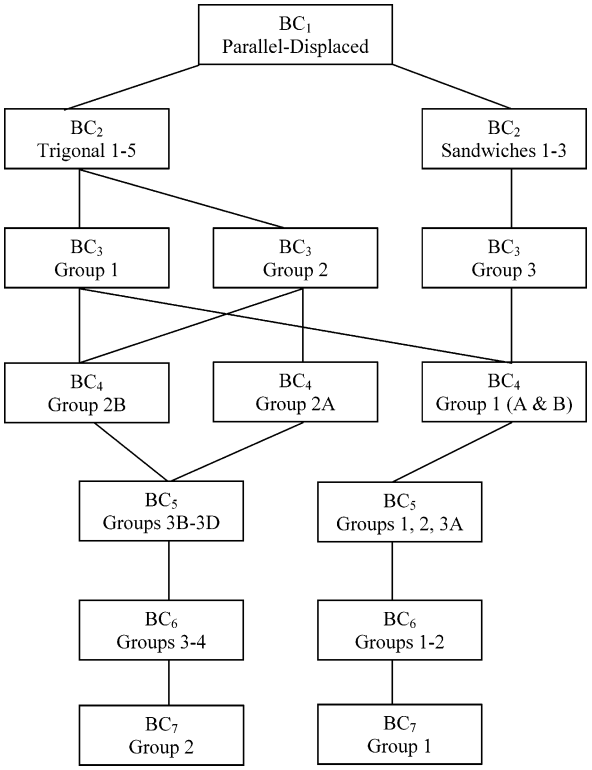

Figure 8. Structural connections between BC_n and BC_{n+1} clusters. Connections between subgroups indicate that the BC_{n+1} structure can be generated by the addition of one cyclohexane to the BC_n structure, when accompanied by translation and reorientation of the original BC_n molecules.

respectively. All of the BC_4 structures are reasonably close to a trigonal bipyramid: The benzene molecule occupies an equatorial position in subgroups 1A, 1B, and 2B (74%) and an axial position in subgroup 2A (26%). The 27% of BC_5 clusters belonging to subgroups 3A and 3B have octahedral-like structures, and the 19% in subgroups 3C and 3D are somewhat similar to the model structure. None of the BC_6 clusters is a tight match to the pentagonal bipyramid structure; however, the 30% of structures in subgroups 1A, 1B, 2A, 3A, 4A, and 4B are somewhat close. Of these, half put benzene in an axial position (subgroups 1A, 2A, and 4A), and half in an equatorial position (subgroups 1B, 3A, and 4B). None of the BC_7 clusters resembles a hexagonal bipyramid. The 30% of BC_{12} clusters belonging to Group 1 mimic an icosahedron, with the 12 cyclohexane molecules forming a complete shell that completely solvates the benzene moiety. Furthermore, C_6H_6 shows a clear nonrandom preference for the interior site of BC_{12}. This preference, not observed in smaller BC_n clusters, is probably related to the relative compactness of the benzene molecule—effecting a better physical fit inside the cluster center.

Van der Waals (vdW) clusters built from spherically symmetric atoms (e.g., Ar) assume minimum-energy structures that can be predicted by maximizing the effectiveness of nearest-neighbor interactions. The present study reveals that only a fraction of BC_n cluster isomers assume structures that are similar to the Ar_n cluster models. The percentage increases from 62% for BC_2 to 89% for BC_3 and maximizes at 100% for BC_4. Thereafter, the percentage decreases to 46% in BC_5, 30% in BC_6, and then to 0% for BC_7. For BC_{12}, where the model predicts a closed-shell icosahedron, 30% of isomers have structures similar to the model.

In this context, it is important to emphasize that approximate conformity to the same model by two different isomers does not necessarily imply other similarities between the two. Consider, for example, the three structural subgroups of BC_6 that approximate a pentagonal bipyramid with benzene in an equatorial position. Of the three, subgroup 1B has a benzene stabilization ratio of 98%, which contrasts with corresponding ratios of ~65% for subgroups 3A and 4B. While C_6H_6 is equatorial, it experiences a substantially different environment in the three isomers. Because the chromophore's local environment differs for each isomer, we do not expect to identify a single peak in the ultraviolet BC_6 spectrum that can be assigned to represent all clusters possessing an equatorial benzene molecule.

IV.C. Relation to Experiment. Easter and Davis reported one-color resonant two-photon ionization spectra for BC_n clusters, $n = 1-10$, measured through benzene's $B_{2u} \leftarrow A_{1g}$ 6_0^1 transition near 260 nm.[21] We observed a BC_3 spectrum dominated by a van der Waals (vdW) progression consisting of six peaks, most having multiplet splitting. Analyzed as a single progression, the vibronic origin was identified at a spectral shift—relative to the molecular C_6H_6 6_0^1 transition—of -136.6 cm^{-1}; the van der Waals fundamental and anharmonicity were determined to be 10.6 and -0.7 cm^{-1}, respectively.[21]

It is possible that a low-frequency vdW mode, with a fundamental frequency near 10 cm^{-1}, is common to each of the major BC_3 isomers represented in the spectrum. If true, then the observed multiplet (quartet or higher) splitting could originate from coexisting isomers, each with slightly different origins and fundamental frequencies. In addition, it is conceivable that the -136.6 cm^{-1} transition origin corresponds to one group (e.g., Group 3), with the other groups (e.g., Groups 1 and 2) having nearly the same van der Waals frequency (~10.5 cm^{-1}) but with origins blue-shifted by either 10.5 or 21 cm^{-1} relative to the Group 3 origin. Such accidental overlap would give the appearance of a single vdW progression with multiplet splitting.

From these comments it must not be inferred that the spectral shift is required in any fundamental way to be proportional to benzene's stabilization energy in the isomer; in fact, the shift reflects zero-point differences between the excited and the ground states. Nevertheless, the spectral intensity of the peak at -136.6 cm^{-1} and the calculated ratios of isomeric structures in our simulations empirically support the second hypothesis.

The spectral shifts of aromatic molecule−rare gas clusters (MA_n) have been interpreted in the literature in a simple manner. General interpretation principles are summarized as follows from ref 27: (1) The spectral shifts induced by rare gas atoms (A) are toward lower energy (red shift); (2) the spectral shift induced by a single rare gas atom is nearly linearly dependent on the polarizability of A; (3) MA_n clusters exhibit several spectroscopic features for a given n, assignable to van der Waals vibrations and electronic origins of different isomers; (4) spectral shifts are not additive per added rare-gas atom (The wording is from ref 27. In context, we interpret the statement as meaning that one cannot simply multiply the number of Ar atoms by a single, fixed per-atom shift value to obtain the cluster's total red shift.); (5) with increasing size, n, spectral features originating from different isomers overlap, resulting in inhomogeneously broadened spectral features; (6) at large enough n, the inhomogeneously broadened feature converges to the bulk value.[27]

This model has been simplified and applied with some success to benzene−argon clusters by incorporating the following additivity assumptions (see ref 29). (1) For one-sided (C_6H_6)-Ar_n structures, the first Ar atom is usually located near the C_6

benzene axis, and additional Ar atoms ($2 \leq n \leq 7$) occupy six successive and equivalent peripheral sites above the gaps formed by two adjacent hydrogen atoms. In these (centered) structures, the most central Ar atom is deemed mainly responsible for the shift observed, with each successive peripheral Ar atom (none of which fundamentally alters the cluster structure) accounting for a small additional blue shift of $\sim$3 cm^{-1}.[28] One-sided structures may also be formed with all symmetrically positioned Ar atoms (none in the center), resulting in decreased spectral shifts compared to the corresponding centered isomers.[29] (2) For two-sided $(C_6H_6)Ar_n$ structures, each side of the C_6H_6 molecule is considered and treated separately. The total spectral shift is then calculated as the simple sum of independent contributions from the two sides; this is referred to as the additivity rule.[30] (3) Structures in which Ar atoms are positioned in the plane defined by the benzene molecule (i.e., equatorial or bridging atoms) are never expected for $(C_6H_6)Ar_n$ with $n < 5$. For larger sizes, the presence of in-plane bridging Ar atoms affects an additional red shift, resulting in experimental spectra that do not follow the simple additivity rule The extent of the red shift in such cases has not been quantified.[29] For the purpose of the discussion that follows, we will refer to this scheme of interpretation for $(C_6H_6)Ar_n$ clusters as the additivity model.

If one assumes that C_6H_{12} can be modeled as an oversized, irregularly shaped argon atom, then one might attempt to assign the $(C_6H_6)(C_6H_{12})_n$ spectra[21] via the additivity model. For the dimer ($n = 1$), the cyclohexane moiety is calculated to assume a parallel-displaced (axial) orientation and has an experimental red shift of 72.3 cm^{-1}.[21,22] For the trimer ($n = 2$), two progressions are observed with red shifts of 65.7 and 57.8 cm^{-1}, respectively. The experimental resolution for all cluster spectra was 0.75 cm^{-1}.[21,22] According to the additivity model, the overall effect of adding a second cyclohexane molecule on the same side of the cluster is to bring a small blue shift relative to the dimer; this is generally consistent with the trigonal isomeric forms identified in ref 22, all of which are "one-sided" and have an axial C_6H_{12}; three BC_2 isomers contain one equatorial (bridging) C_6H_{12}—which crosses the $x-y$ plane—while the other two have a cyclohexane moiety that is intermediate between axial and equatorial and is entirely above the plane. (This assignment from the additivity model, if correct, differs from the assignment originally proposed in ref 22.) It is important to note that the relative positions and orientations of axial molecules in the trigonal trimers differ from each other and also from those of the dimer and cannot be viewed as equivalent. We also note that the additivity model would require a hypothetical red shift near 145 cm^{-1} for assignment to any of the three (calculated) higher-energy sandwich dimers;[22] such a shift is not observed in the spectrum.

The tetramer ($n = 3$) has a transition origin red-shifted by 136.6 cm^{-1}.[21] The experimental shift is not greatly different from the sum of 72.3 cm^{-1} (dimer) + 65.7 cm^{-1} (trimer); therefore, the additivity model would assign a two-sided form. Isomer 2 (modified sandwich) is the only structure calculated in our studies that has cyclohexane centers of mass on both sides of benzene. The way to reconcile our study with the additivity model is to hypothesize that both axial cyclohexanes contribute 72 cm^{-1} to the red shift, with the vertical equatorial cyclohexane molecule affecting an additional blue shift of 8 cm^{-1}. This assignment is not completely satisfactory, however, because (1) it fails to account for the observed multiplet (quartet or higher) splitting in the spectra and (2) it fails to account for the presence of any one-sided tetramer isomers, which are so prevalent in our results.

Extended to the pentamer, $n = 4$, where the primary feature in the R2PI spectrum has a red shift near 40 cm^{-1}, the additivity model would assign a one-sided structure with no cyclohexanes occupying a parallel-displaced position above benzene. BC_4 structures of Groups 2A and 2B share these characteristics.

Clearly, the additivity model—which has been used with some success to interpret benzene−argon cluster spectra—is only partially satisfactory for making assignments consistent with our MC results. It would be incorrect to conclude from this that one or the other is fundamentally incorrect. Plainly, the cyclohexane molecule is not argon-like: It is neither compact nor spherically symmetric. It occupies significantly more volume than Ar and consists of 12 partially positive hydrogen atoms surrounding six partially negative carbon atoms. It is obvious that cyclohexane cannot pack around benzene in the same fashion as argon. Even in the dimer, the cyclohexane is not centered about the z-axis,[22] and the notion of seating seven cyclohexane molecules on the same size of a benzene molecule—one in the central position and six in equivalent positions between hydrogen atoms—is unthinkable. To make things more complex, the relative orientation of each cyclohexane molecule, with respect both to benzene and to the other cyclohexane molecules present, is critical for BC_n, whereas for small benzene−argon clusters the orientation of Ar is irrelevant. Finally, equatorial cyclohexane molecules (i.e., in which a portion of the cyclohexane crosses the $x-y$ plane) are common in small BC_n clusters, whereas bridging argon atoms are unknown in smaller BA_n clusters.

In short, the simplicity of the additivity model for benzene−argon cluster spectra relies heavily on the compactness and spherical symmetry of the argon moieties and their ability to pack in well-defined symmetry-related sites on the benzene surface. Cyclohexane differs fundamentally from Ar because of its size and shape, it breaks the $x-y$ plane in many structures, and orientation plays a significant role on intermolecular interaction energies, rendering it impossible to predefine specific sites on benzene where a cyclohexane moiety must attach itself. Furthermore, cyclohexane−cyclohexane interactions play a far more important role in determining low-energy structures than corresponding argon−argon interactions in equal-size BAr_n clusters. Consequently, the additivity model would have to be modified, taking these complexities into account, to fully and adequately describe BC_n clusters. Such a modification of the model is beyond the scope of this report.

To further assess our results, MP2 calculations (optimization and energy) were carried out on three initial tetramer structures: Isomer 2, Isomer 3, and a hypothetical isomer, H2 (described below). In preparation, three hypothetical two-sided structures were created that are consistent with possible expectations of the additivity model described above. To create the structures, the cyclohexane molecular coordinates of BC_1 on one side of benzene were combined (in three different orientations) with those of the one-sided BC_2 Trigonal 3 Isomer (ref 22) on the other side. This yielded three two-sided starting structures containing no cyclohexane molecules that breach the $x-y$ plane. Initial structures were then optimized to 0.001 K several times on all four PESs, resulting in the identification of three hypothetical isomers (H1−H3; Figure S3 and Tables S62−S64). Each hypothetical isomer was verified to occupy a local minimum all four PESs. Of the three, only H2 spontaneously rearranged into a different structure (H1) during isothermal simulations at 5 K on the Shi PES. All four PESs predict the lowest-energy hypothetical two-sided (H1) isomer to be 5 kJ/mol higher in energy than Isomer 3 (Table 8), which is

TABLE 8: Relative Optimized Energies of Tetramer Isomers 2 and 3 and a Hypothetical Two-Sided Tetramer Isomer

	relative energies (kJ mol^{-1})		
	Isomer 2 trigonal	Isomer 3 sandwich	Isomer H1 two-sided
Jorgensen MC	1.2	0.0	5.7
Shi MC	1.1	0.0	5.5
van de Waal MC	0.8	0.0	4.9
Williams MC	0.7	0.0	5.1
MP2/6-31g(d)	0.0	0.5	4.4

significantly larger than kT at 10 K (0.083 kJ mol^{-1}). The MP2 calculations confirm this result qualitatively, with the hypothetical cluster's relative MP2 energy being $\sim 50kT$ higher than the lowest-energy MP2 major isomer at 10 K.

The MP2/6-31g(d) calculations represent the highest level of theory achievable on the tetramer with the hardware/software configuration available. In comparison to MC results, MP2 energies are reversed for Isomers 2 and 3, with a relative shift between the two between 1.2 and 1.7 kJ mol^{-1}; in addition, the energy of isomer H1 is improved in the MP2 calculation relative to that of Isomer 3 by approximately the same amount, i.e., 1.0−1.8 kJ mol^{-1}. It has been documented that MP2/6-31g* calculations on the benzene dimer overestimate the binding energy of the parallel-displaced arrangement structure compared to that of the T-shaped geometry.[31] Although cyclohexane lacks a π-electron system and the two cluster systems are clearly not equivalent, it is nevertheless possible that the MP2 calculation overestimates the binding stabilization of parallel benzene−cyclohexane interactions relative to T-type interactions in BC_n clusters as well. If this is true, then Isomer 3's energy, relative to those of Isomers 2 and H1, could easily be 1−2 kJ mol^{-1} more favorable than the MP2 values indicate, consistent with our MC calculations. In this context, it is also necessary to recognize that the MP2 energy differences between structural isomers can have associated errors on the order of 1 kcal mol^{-1}. Because this potential error is not significantly smaller than the calculated MP2 energy differences in Table 8, it is fair to conclude that the MP2 results—by themselves—are insufficient to establish the relative energy ordering among the isomers. The value of the MP2 results is that they are independent of and appear to offer qualitative support for the MC calculation results.

In their report, El-Shall and Whetten tentatively assigned two sharp features in the BC_6 spectrum to C_6H_6 occupying an axial or equatorial position within a pentagonal bipyramid structure.[20] Results of this study cast some doubt on those assignments. First, only ~30% of BC_6 cluster structures are loosely described as pentagonal bipyramidal; half of these have C_6H_6 in an axial position, and the other half in an equatorial position. The situation is further complicated by the fact that axial benzene is present in three different subgroups; equatorial benzene is also present in three other subgroups. Within the "axial" subgroups, the benzene stabilization energy ranges from 65% to 97%, and the corresponding range for "equatorial" benzenes is 64% to 98%. On the basis of these findings, it is unlikely that either "axial" or "equatorial" benzenes are separately represented by single sharp features in the 6_0^1 BC_6 spectrum. We here re-emphasize that the experimental red shift depends on differences in the ground and excited states, and their magnitude is not directly related to benzene stabilization energies in a straightforward manner. Nevertheless, differences in the benzene stabilization energy indicate differences in local environment, which should give rise to different transitions and distinct spectral features, barring accidental degeneracy.

A final comment is in order. The MP2 calculations may indicate that the energy difference between Group 1 and Group 2 isomers is relatively small and that the ordering may (though not certain) be inverted in our MCSA results. Hypothetically, the ordering could be affected by changing the algebraic formula used for assigning partial charges to hydrogen atoms, $q_H = Ce/(n+1)$, where C is a constant for the PES, e is the fundamental charge, and n represents the number of hydrogen atoms in the molecule's $-(CH_n)-$ groups.[16,23] The effect of changing the partial-charge formula in the PESs would be to alter the relative energies of solvent−solute versus solute−solute interactions. However, even if the energy ordering between the one-sided and the bridged isomers were hypothetically reversed, then two other results would still need to be observed in simulations using the modified PESs for them to be consistent with assignments based on the additivity model in its present form. (1) One or more new bridged isomers would have to be identified to explain the experimental spectrum, which contains multiplet (quartet or higher) splitting. (2) The ratio of Group 3 isomers identified in the simulations (~11% in our work), which reflects the approximate population of such isomers in the experiment, would have to increase significantly. While such results cannot be ruled out without performing additional studies, it appears likely that the additivity model will need to be more fully developed—extended to included nonpolar polyatomic molecules—before it can fully and unambiguously assign features in the BC_n R2PI spectra.

IV.D. Isomerization in the Tetramer. The caloric studies of the five major BC_3 isomers clearly separate Isomer 2 (modified sandwich) from the others (quasi-tetrahedral), with a barrier that prevents isomerization at temperatures below 50 K. Our isothermal data also reveal that trigonal Isomers 1 and 3−5 are distinct and occupy separate local minima on the PES at 5 K. Isomerization barriers are presumed to be small between these isomeric forms, but further quantification is not possible.

IV.E. Appropriateness of the MCSA Methodology and the Influence of the PES. Recently, state-of-the-art global minimization methods have been developed, including genetic algorithms,[32] Monte Carlo plus minimization,[33] parallel tempering Monte Carlo,[34] and a new heuristic and unbiased method by Takeuchi.[35] These approaches are regarded as efficient for optimizing van der Waals clusters to global minima. The MCSA methodology that we have employed in this study has been criticized because individual simulations often result in the identification of local (but not global) energy minima; furthermore, multiple simulations are required to identify and confirm global minima.

It is important to emphasize in this context that "more efficient" does not imply "more accurate". Our recent MCSA calculations on $(C_6H_6)_{13}$ clusters[12,13] have either verified previous results[15] or improved upon them.[16,18,36] Furthermore, a recent state-of-the-art optimization study has only confirmed our published results but could not improve upon them.[35] The minimum energies and related structures that we report are consistently reproducible.

Furthermore, it must be emphasized that a perceived "weakness" of the method actually benefits this study. The MCSA method has been faulted because many simulations end in local, nonglobal minima. For our purposes this "deficiency" is a bonus. From previous work, it is clear that the formation of molecular cluster structures (isomers) in supersonic jets is governed primarily by kinetic not thermodynamic influences.[12,21] To the extent that the PESs used mimic physical reality, the ratio of isomers identified in our simulations reflects the approximate

ratio of isomers present in experimental expansions. Understanding these ratios is crucial to the interpretation of R2PI spectra.

IV.F. Influence of the PES. In these studies, we have used four different PESs for the purpose of identifying local minimum energy structures, with the goal of minimizing artifacts originating from any one PES. We find it remarkable that all four PESs are in such strong agreement regarding their predictions of structures and properties for B_{13},[12] BC_1 and BC_2,[22] and BC_3 (section III.A).

In the B_{13} studies, all four PESs predict the same two lowest-energy isomers within small confidence limits. Specifically, the 95% confidence limits of the two composite structures for either isomer (averaged over the four PESs) are never larger than (0.12 Å, 0.011, 0.030, 0.036, 0.032, 0.039) for the molecular coordinates (r, Θ Φ, α, β, γ), where angles are in radians.[12] Expectedly, absolute energies do differ somewhat, with the magnitudes of absolute cluster stabilization energies decreasing as follows: $E_{\text{Shi}} > E_{\text{Williams}} > E_{\text{van de Waal}} > E_{\text{Jorgensen}}$. The most noteworthy differences in the B_{13} results are two: (1) One isomer (A) is identified as the global minimum by all except the Jorgensen PES; (2) the Williams PES attributes S_6 symmetry to isomer A, while the other three PESs predict C_3 symmetry. For all four PESs, isomer B is attributed with C_3 symmetry. The energy differences between the two isomers (A and B) are as follows: Williams $= -0.60$ kJ mol^{-1} (0.18%); van de Waal $= -0.98$ kJ mol^{-1} (0.30%); Shi $= -0.24$ kJ mol^{-1} (0.07%); Jorgensen $= +0.86$ kJ mol^{-1} (-0.27%)—where the percent (in parentheses) indicates the difference relative to the absolute energy of Isomer A on the same PES. Clearly, all such differences are very small.

In the BC_1 and BC_2 studies, the PES ordering of total cluster stabilization energy differs from that of B_{13}: $E_{\text{Jorgensen}} > E_{\text{Williams}} \geq E_{\text{van de Waal}} > E_{\text{Shi}}$.[22] All four PESs unanimously predict a single parallel-displaced dimer structure, with the maximum $\langle(\Delta r/A)^2\rangle$ value between an individual PES (van de Waal) and the mean composite structure being 0.0148, indicating a root-mean-square (rms) displacement of no more than 0.12 Å, evaluated over all 18 cyclohexane carbon and hydrogen atomic coordinates in the structure. Caloric studies on the dimer (ref 22; Figures 3 and 4) also demonstrate that trajectories averaged over all four PESs at 1 K resolution and plotted on a relative energy scale (as in Figure 3 of this report) provide information indistinguishable from that of a single PES (Jorgensen) simulation at 0.1 K resolution.

In the BC_2 trimer studies, minor variations are observed between the PESs. For example, the energy ordering of Trigonal Isomers 1, 2, 3, and 5 differs for the Shi and van de Waal PESs, compared to the mean ordering (which is the same as that of the Jorgensen and Williams PESs). Specifically, while the mean ordering of these isomers is 5 > 1 > 2 > 3, that of Shi is 1 > 2 > 5 > 3, and that of van de Waal is 5 > 2 > 3 > 1. On the basis of relative energies (calculated with reference to the Trigonal 4 isomer—the global minimum on all four PESs), the average and standard deviations of the four trigonal isomer relative energies (5, 1, 2, 3) are (0.987 ± 0.008, 0.983 ± 0.002, 0.979 ± 0.013, 0.974 ± 0.012). The 95% confidence limit of the difference between any two isomer energies (Δ_D) is given by $\Delta_D = t_{95,\nu} S_{12}(1/N_1 + 1/N_2)^{1/2}$, where $S_{12} = \sqrt{((N_1-1))S_1^2+((N_2-1))S_2^2/N_1+N_2-2}$. Here, $N_1 = N_2 = 4$, and the value of the Student t distribution parameter, $t_{95,\nu=6} = 2.45$ ($\nu = 6$ degrees of freedom). In all pairwise cases, the energy difference between isomers is smaller than Δ_D. Thus, variations among the four PESs are not statistically meaningful. Thus, even though relative stabilities of the four trigonal isomers cannot be assigned unambiguously, the implementation of average relative energies is useful for purposes of comparison.

Minor PES-related differences are also observed in the BC_3 tetramer results, reported in section III.A. (1) Absolute values of cluster stabilization energies follow the same trend as for BC_1 and BC_2: $E_{\text{Jorgensen}} > E_{\text{Williams}} > E_{\text{van de Waal}} > E_{\text{Shi}}$. (2) The Jorgensen and Williams PESs predict Isomer 1 to be lower in energy than Isomer 3 by 0.11 and 0.07 kJ mol^{-1}, respectively, with relative energy differences of 0.19% and 0.14% between the isomers. The Shi and van de Waal PESs reverse the order, with energy differences of 0.20 and 0.07 kJ mol^{-1}, respectively, corresponding to relative differences 0.41% and 0.14%. (3) The optimized structure of Isomer 1A predicted by Jorgensen and Shi differs slightly from that of Williams and van de Waal (1B), with a relative $\langle(\Delta r/A)^2\rangle$ value of 0.27, indicating an rms deviation of 0.5 Å in the 54 cyclohexane atomic coordinates. (4) Approximately 20% of the Williams and van de Waal simulations on BC_3 resulted in high-symmetry Group 3 (modified sandwich) tetramer structures, compared to 5% and 0%, respectively, for simulations on the Shi and Jorgensen PESs. (5) Three of the minor tetramer isomers (Tables S56−S59) do not occupy relative minima on one or more PES: Isomer 6 is found on neither the Williams nor Jorgensen PESs, and local minima corresponding to Isomers 7−8 are not identified by the Jorgensen PES.

In summary, it is unsurprising that individual PESs have slight differences in their predictions. Most such differences are minor, and the data do not permit a systematic statement of how these differences will affect other calculations. Two points are worth noting, however. (1). Within the same system (e.g., BC_n), the ordering of absolute calculated energies appears to follow a single pattern, $E_{\text{Jorgensen}} > E_{\text{Williams}} \geq E_{\text{van de Waal}} > E_{\text{Shi}}$. However, the order is not universal and differs for other systems (e.g., B_n). This punctuates the importance of analyzing energies as relative energies on the relevant PES and of correlating multiple PES results to minimize artifacts originating from a single PES. (2). It is possible (though not proved by these data) that the exp 6−1 form of the Williams PES favors higher symmetry in its minimum energy structures, compared to the 12−6−1 functional form of the other three PESs. For example, the Williams PES predicts S_6 symmetry for B_{13} isomer A, compared to the C_3 symmetry predicted by the three 12−6−1 PESs. Furthermore, simulations of the tetramer, BC_3, on the Williams PES result in a higher percentage of Group 3 structures than either the Shi or Jorgensen PES, although they match the percentages derived from the van de Waal PES. Further studies will be necessary for confirmation of this possible trend.

V. Conclusions

Five primary conclusions result from this investigation. (1) BC_3 is the largest BC_n cluster that exists in few enough isomeric forms to permit the isomers to be uniquely identified and characterized. Of the five major BC_3 isomers, one assumes a symmetric, modified-sandwich arrangement. The other four are more tetrahedral in arrangement but lack specific symmetry. (2) Isomers of BC_4 and larger clusters can be classified on the basis of common structural characteristics. Although the classification scheme developed in this report contains arbitrary elements, it provides a foundation for assessing relationships between adjacent-size clusters. (3) Two major, parallel tracks have been identified that describe the evolution of cluster structures as a function of size (Figure 8). These are proposed to represent primary pathways followed when (a) BC_{n+1} is built

from a rigid BC_n cluster by addition of one cyclohexane or (b) BC_n is formed by evaporation of one cyclohexane from a rigid BC_{n+1} structure. In almost all cases, the addition (or evaporation) of a cyclohexane molecule must be accompanied by translation and/or reorientation of existing cluster members. The two evolutionary tracks are generally isolated, although they are connected between BC_3 and BC_4. One track tends to maximize solvation of the benzene moiety, while the other tends to maximize cyclohexane−cyclohexane interactions and pushes benzene to the cluster surface. (4) Only a fraction of BC_n clusters assume structures mimicking those predicted for neat rare-gas clusters. The fractions are larger for small clusters (to BC_4) but rapidly decrease for larger sizes. In BC_{12}, where a closed-shell structure is expected, the fraction increases to 30%. Due to the plethora of isomers, it is improbable that experimental spectra are amenable to a straightforward interpretation in terms of specific sites within rigid clusters for clusters larger than BC_3. (5) The R2PI spectra can only be partially understood in terms of the additivity model, which—to be unambiguous—will require refinements that extend to nonpolar polyatomic molecular solvents.

Computational and experimental studies of neat benzene clusters have historically been based on single isomeric structures for each size, with the exception of B_{13}, which is known to coexist in two low-energy isomeric forms.[12] This historical emphasis contrasts with our present findings for BC_n clusters: A single isomer is identified for BC_1, eight for BC_2, five major isomers for BC_3, and a large, unknown number of isomers for BC_4 and larger. Additional comprehensive studies of neat B_n and C_n clusters may clarify the extent to which isomerization originates from symmetry-breaking within the seeded BC_n cluster. Experimentation with the algebraic formula used to assign atomic partial charges in the PESs would affect relative strengths of solvent−solute and solvent−solvent interactions that could affect isomer energies, structures, and their predicted relative populations in experimental supersonic expansions.

Appendix

Potential Energy Surfaces. Four different nonbonded pair potential energy functions are used in our $(C_6H_6)(C_6H_{12})_n$ simulations, derived from the work of Williams and Starr,[23] van de Waal,[16] Shi and Bartell,[24] and Jorgensen and Severance.[25] In previous modeling of neat benzene clusters, we adapted several authors' original interaction parameters to a common functional form

$$V_{ij}(r) = C_{\text{pre}} \exp(-C_{\text{exp}} r_{ij}) + C_{12} r_{ij}^{-12} + C_6 r_{ij}^{-6} + C_1 r_{ij}^{-1}$$

where r_{ij} is the distance between atoms i and j.[12,13] Using our adapted parameters, potential energies are calculated in units of kJ mol^{-1} when distances are in angstroms. For neat benzene simulations, three separate sets of parameters are required, corresponding to each of the three interactions: C−C, C−H, and H−H. With benzene and cyclohexane molecules simultaneously present in the cluster, the original PES parameters must be adapted to include C_6H_{12}, which has unique bond lengths and partial atomic charges associated with its atoms. Potential energy parameters and their corresponding molecular bond distances are provided in the tables that follow Note that all tables containing A in their identification label are located in the Appendix (e.g., Table A4).

The primary difference from the parameters tabulated in ref 12 is that we tabulate only the absolute value of C_1, specific to benzene−benzene interactions (Tables A1, A4, A5, and A7).

TABLE A1: Potential Energy Parameters for the Williams exp 6−1 PES[a]

Williams	C_{pre}	C_{exp}	C_6	$\lvert C_1\rvert$ (C_6H_6)
C−C	367 250	3.60	−2414	
C−H	65 485	3.67	−573	
H−H	11 677	3.74	−136	32.523

[a] The C_1 coefficient in the last column applies only to benzene−benzene interactions; other parameters are applicable to interactions in mixtures of hydrocarbons.

TABLE A2: Relative Atomic Charges in Benzene and Cyclohexane[a]

C_1/C_1(H−H, C_6H_6)	C (C_6H_6) (−1)	H (C_6H_6) (+1)	C (C_6H_{12}) ($-^4/_3$)	H (C_6H_{12}) ($+^2/_3$)
C (C_6H_6) (−1)	1	−1	$+^4/_3$	$-^2/_3$
H (C_6H_6) (+1)		+1	$-^4/_3$	$+^2/_3$
C (C_6H_{12}) ($-^4/_3$)			$+^{16}/_9$	$-^8/_9$
H (C_6H_{12}) ($+^2/_3$)				$+^4/_9$

[a] The column and row headings identify the four kinds of atoms and their relative charges. Individual entries in the table indicate the factor that must be multiplied by the C_1 entry in Table 1 to obtain the correct C_1 coefficient for each pairwise interaction. Only the last two columns are needed for $(C_6H_6)(C_6H_{12})_n$ clusters, which have no benzene−benzene interactions

TABLE A3: Atomic Coordinates and Bond Distances for the Williams and Van de Waal Potential Energy Surfaces[a]

Williams and van de Waal	x (Å)	y (Å)	z (Å)	bonded pair	bond distance (Å)
C_1(B)	1.3970	0.0000	0.0000	C−C(B)	1.397
H_1(B)	2.4240	0.0000	0.0000	C−H(B)	1.027
C_1(C)	1.4387	0.0000	0.2543	C−C(C)	1.526
H_{1e}(C)	2.4193	0.0000	−0.0923	C−H_e(C)	1.040
H_{7a}(C)	1.4387	0.0000	1.2943	C−H_a(C)	1.040

[a] Cartesian coordinates are indicated for five symmetry-unique atoms with the molecule in its reference orientation. Coordinates are generated from the bond distances assumed by the PES, based on the assumption that cyclohexane's bond angles are tetrahedral.

TABLE A4: Parameters of the van de Waal 12−6−1 Potential Energy Surface

Van de Waal	C_{12}	C_6	$\lvert C_1\rvert$ (C_6H_6)
C−C	4 869 316	−2765.3	
C−H	681 906	−625.6	
H−H	89 476	−139.4	32.523

TABLE A5: Parameters of the Shi(3) 12−6−1 Potential Energy Surface

Shi(3)	C_{12}	C_6	$\lvert C_1\rvert$ (C_6H_6)
C−C	2 899 300	−2291.0	
C−H	369 090	−433.9	
H−H	21 010	−66.2	30.13

$|C_1|$ is then multiplied by the appropriate factor (Table A2) to obtain the C_1 parameter for a specific atom−atom interaction. This follows the approach of Williams and Starr.[23] Their original C_1 coefficients were based on the assumption that for neutral hydrocarbons hydrogen atoms can be assigned atomic charges, $q_H = 0.306e/n + 1$, where n represents the number of hydrogen atoms in the molecule's $-(CH_n)-$ groups.[16,23] For benzene, hydrogen's atomic charge is proportional to $^1/_2e$ ($n = 1$), whereas for cyclohexane the charge is proportional to $^1/_3e$ ($n = 2$). Consequently, the hydrogenic charge in cyclohexane is $^2/_3$ of the corresponding value in benzene. Molecular neutrality demands that the charge on the carbon atom is proportional to $-^1/_2e$ in benzene and to $-^2/_3e$ in cyclohexane. In Table A2, each of the four kinds of atoms is indicated in both the column and the row headings, along with its relative charge. Tabulated

TABLE A6: Atomic Coordinates and Bond Distances for the Shi(3) PES

Shi(3)	*x* (Å)	*y* (Å)	*z* (Å)	bonded pair	bond distance (Å)
C_1(B)	1.4010	0.0000	0.0000	C−C(B)	1.401
H_1(B)	2.4320	0.0000	0.0000	C−H(B)	1.031
C_1(C)	1.4519	0.0000	0.2567	C−C(C)	1.540[a]
H_{1e}(C)	2.4325	0.0000	−0.0900	C−He(C)	1.040[a]
H_{7a}(C)	1.4519	0.0000	1.2967	C−H_a(C)	1.040[a]

[a] The bond distances for cyclohexane were not included in the original model and were assigned as described in the text.

TABLE A7: Parameters of the Jorgensen 12−6−1 Potential Energy Surface

Jorgensen	C_{12}	C_6	$\|C_1\|$ (C_6H_6)
C−C	4 693 425.7	−2344.9	
C−H	308 335.8	−486.2	
H−H	20 256.2	−100.8	18.37

TABLE A8: Atomic Coordinates and Bond Distances for the Jorgensen Potential Energy Surface

Jorgensen	*x* (Å)	*y* (Å)	*z* (Å)	bonded pair	bond distance (Å)
C_1(B)	1.4000	0.0000	0.0000	C−C(B)	1.400
H_1(B)	2.4800	0.0000	0.0000	C−H(B)	1.080
C_1(C)	1.4519	0.0000	0.2567	C−C(C)	1.540[a]
H_{1e}(C)	2.4796	0.0000	−0.1067	C−H_e(C)	1.090[a]
H_{7a}(C)	1.4519	0.0000	1.3467	C−H_a(C)	1.090[a]

[a] The bond distances for cyclohexane were not included in the original model and are assumed to be standard.

entries are the products of contributing relative atomic charges; therefore, tabulated coefficients must be multiplied by the value of $|C_1|$ (C_6H_6) to obtain the correct C_1 coefficient for a given atom−atom interaction.

The Cartesian coordinates of five atoms in their reference orientations are also provided in Tables A3, A6, and A7. Because bond distances for cyclohexane were not available from refs 24 or 25, the distances were chosen to reflect the original authors' choice for benzene: Distances are assumed to be standard for the Jorgensen potential; for the Shi and Bartell surface, the C−C bond is taken as standard, but the C−H bond is foreshortened to compensate for the asphericity of the hydrogen atoms.[24]

Acknowledgment. This work was partially supported by the ACS Petroleum Research Fund (Grant No. 42148-B6). David Terrell contributed to preliminary calculations on BC_3 and BC_5. Both J.A.R. and L.J.B. were partially supported via summer stipends from the PRF Grant.

Supporting Information Available: Detailed information on the structures and energies of BC_n isomers, including BC_3 (major, minor, and hypothetical isomers), BC_4−BC_7, and BC_{12} and a detailed analysis and description of the structural grouping, with group properties and energies of BC_5 (section S.I.), BC_6 (section S.II.), BC_7 (section S.III.), and BC_{12} (section S.IV.). This material is available free of charge via the Internet at http://pubs.acs.org.

References and Notes

(1) Bornsen, K. O.; Lin, S. H.; Selzle, H. L.; Schlag, E. W. *J. Chem. Phys.* **1989**, *90*, 1299.
(2) Easter, D. C.; Harris, J. P.; Langendorf, M.; Mellott, J.; Neel, M.; Weiss, T. *J. Phys. Chem. A* **1998**, *102*, 10032.
(3) Easter, D. C.; Baronavski, A. P.; Hawley, M. *J. Chem. Phys.* **1993**, *99*, 4942.
(4) Easter, D. C.; Khoury, J. T.; Whetten, R. L. *J. Chem. Phys.* **1992**, *97*, 1675.
(5) Easter, D. C.; Li, X.; Whetten, R. L. *J. Chem. Phys.* **1991**, *95*, 6362.
(6) Easter, D. C.; Whetten, R. L.; Wessel, J. E. *J. Chem. Phys.* **1991**, *94*, 3347.
(7) Bornsen, K. O.; Selzle, H. L.; Schlag, E. W. *J. Chem. Phys.* **1986**, *85*, 1726.
(8) Schlag, E. W.; Selzle, H. L. *J. Chem. Soc., Faraday Trans.* **1990**, *86*, 2511.
(9) Iimori, T.; Aoki, Y.; Ohshima, Y. *J. Chem. Phys.* **2002**, *117*, 3675.
(10) Iimori, T.; Ohshima, Y. *J. Chem. Phys.* **2001**, *114*, 2867.
(11) Iimori, T.; Ohshima, Y. *J. Chem. Phys.* **2002**, *117*, 3656.
(12) Easter, D. C. *J. Phys. Chem. A* **2003**, *107*, 7733.
(13) Easter, D. C. *J. Phys. Chem. A* **2003**, *107*, 2148.
(14) Easter, D. C. *J. Cluster Sci.* **2004**, *15*, 33.
(15) Williams, D. E. *Acta Crystallogr., Sect. A* **1980**, *36*, 715.
(16) Van de Waal, B. W. *J. Chem. Phys.* **1983**, *79*, 3948.
(17) Van de Waal, B. W. *Chem. Phys. Lett.* **1986**, *123*, 69.
(18) Bartell, L. S.; Dulles, F. J. *J. Phys. Chem.* **1995**, *99*, 17107.
(19) Hoare, M. R. *Adv. Chem. Phys.* **1979**, *40*, 49.
(20) El-Shall, M. S.; Whetten, R. L. *Chem. Phys. Lett.* **1989**, *163*, 41.
(21) Easter, D. C.; Davis, K. A. *Chem. Phys. Lett.* **2003**, *380*, 471.
(22) Easter, D. C.; Terrell, D. A.; Roof, J. A. *J. Phys. Chem. A* **2005**, *109*, 673.
(23) Williams, D. E.; Starr, T. L. *Comput. Chem.* **1977**, *1*, 173.
(24) Shi, X. Q.; Bartell, L. S. *J. Phys. Chem.* **1988**, *92*, 5667.
(25) Jorgensen, W. L.; Severance, D. L. *J. Am. Chem. Soc.* **1990**, *112*, 4768.
(26) Frisch, M. J.; Trucks, G. W.; Schlegel, H. B.; Scuseria, G. E.; Robb, M. A.; Cheeseman, J. R.; Montgomery, J. A.; Vreven, T.; Kudin, K. N.; Burant, J. C.; Millam, J. M.; Iyengar, S. S.; Tomasi, J.; Barone, V.; Mennucci, B.; Cossi, M.; Scalmani, G.; Rega, N.; Petersson, G. A.; Nakatsuji, H.; Hada, M.; Ehara, M.; Toyota, K.; Fukuda, R.; Hasegawa, J.; Ishida, M.; Nakajima, T.; Honda, Y.; Kitao, O.; Nakai, H.; Klene, M.; Li, X.; Knox, J. E.; Hratchian, H. P.; Cross, J. B.; Adamo, C.; Jaramillo, J.; Gomperts, R.; Stratmann, R. E.; Yazyev, O.; Austin, A. J.; Cammi, R.; Pomelli, C.; Ochterski, J. W.; Ayala, P. Y.; Morokuma, K.; Voth, G. A.; Salvador, P.; Dannenberg, J. J.; Zakrzewski, V. G.; Dapprich, S.; Daniels, A. D.; Strain, M. C.; Farkas, O.; Malick, D. K.; Rabuck, A. D.; Raghavachari, K.; Foresman, J. B.; Ortiz, J. V.; Cui, Q.; Baboul, A. G.; Clifford, S.; Cioslowski, J.; Stefanov, B. B.; Liu, G.; Liashenko, A.; Piskorz, P.; Komaromi, I.; Martin, R. L.; Fox, D. J.; Keith, T.; Al-Laham, M. A.; Peng, C. Y.; Nanayakkara, A.; Challacombe, M.; Gill, P. M. W.; Johnson, B.; Chen, W.; Wong, M. W.; Gonzalez, C.; Pople, J. A. *Gaussian 03*, revision C.02; Gaussian, Inc.: Wallingford, CT, 2004.
(27) Shalev, E.; Ben-Horin, N.; Even, U.; Jortner, J. *J. Chem. Phys.* **1991**, *95*, 3147.
(28) Schmidt, M.; Mons, M.; Le Calve, J. *J. Phys. Chem.* **1992**, *96*, 2404.
(29) Schmidt, M.; Le Calve, J.; Mons, M. *J. Chem. Phys.* **1993**, *98*, 6102.
(30) Schmidt, M.; Mons, M.; Le Calve, J. *Chem. Phys. Lett.* **1991**, *177*, 371.
(31) Hobza, P.; Selzle, H. L.; Schlag, E. W. *J. Phys. Chem.* **1996**, *100*, 18790.
(32) Kabrede, H.; Hentschke, R. *J. Phys. Chem. B* **2003**, *107*, 3914.
(33) Hodges, M. P.; Wales, D. J. *Chem. Phys. Lett.* **2000**, *324*, 279.
(34) Rapacioli, M.; Calvo, F.; Spiegelman, F.; Joblin, C.; Wales, D. J. *J. Phys. Chem. A* **2005**, *109*, 2487.
(35) Takeuchi, H. *J. Chem. Inf. Model.* **2007**, *47*, 104.
(36) Dulles, F. J.; Bartell, L. S. *J. Phys. Chem.* **1995**, *99*, 17100.